Rev. Mexicana Astron. Astrof., **20**, 85-112 (1990)

THE IUE SPECTRUM OF THE WOLF-RAYET SYSTEM HD 193077

G. Koenigsberger

Instituto de Astronomía
Universidad Nacional Autónoma de México

Received 1990 May 3

RESUMEN

Se presentan los resultados de la identificación de líneas en el espectro *UV* (1100 - 1900) de la estrella Wolf-Rayet (WR) HD 193077 (WR138) obtenido con el IUE. El espectro de líneas en emisión se ve dominado por líneas de Fe V + Fe VI en $\lambda < 1500$ A. El espectro de líneas interestelares contiene una gran variedad de especies atómicas e iónicas, desde C I hasta Si IV y C IV, y también CO. Asociadas a las líneas intensas provenientes de especies ionizadas, se encuentran líneas desplazadas en aproximadamente -45 km s^{-1}. El espectro de líneas en absorción fotosféricas contiene principalmente líneas de Fe V, Fe IV, N IV, N III, C III, Ni IV, Si III, Si II, habiendo un aumento en el ancho total (FWCI) de la línea conforme disminuye el potencial de ionización. El rango de FWCI es de 250 km s^{-1} para las líneas de más alto grado de ionización hasta aproximadamente 1500 km s^{-1} para el hidrógeno, pasando por 800 km s^{-1} para las líneas de menor grado de ionización observadas en el *UV*, lo cual es consistente con la presencia de una estrella que rota muy rápidamente. La evidencia apunta hacia la conclusión, aunque aún no definitiva, que tanto el espectro de líneas en emisión como el de líneas en absorción provienen de la misma estrella.

ABSTRACT

The results of a detailed line-identification study of the IUE (1100 - 1900 A) spectrum of the Wolf-Rayet star HD 193077 (WR138) is presented. The emission line spectrum is shown to be dominated by Fe V + Fe VI lines below 1500 A. The insterstellar- line spectrum contains a large variety of atomic and ionic species, ranging from C I to Si IV and C IV, and CO. Insterstellar features displaced by approximately -45 km s^{-1} are associated with the strong lines arising from the ionized species. The measurable photospheric absorption line spectrum contains lines primarily from Fe V, Fe IV, N IV, N III, C III, Ni IV, Si III, Si II, with an increase in full widths at continuun intensity (FWCI) with decreasing ionization potential. This progression ranges from values of FWCI of 250 km s^{-1} for the highest ionization lines, through 800 km s^{-1} for the lowest ionization lines in the *UV* to approximately 1500 km s^{-1} for hydrogen, and is consistent with a rapidly rotating star. It is pointed out that the photospheric lines originating in the polar region will suffer from limb darkening effects which makes them weaker than would be observed in a non-rotating star of equivalent temperature and gravity, thus providing evidence, though not conclusive, that the emission-line and the photospheric-line spectra arise in the same star.

Key words: **SPECTROSCOPY – STARS-WOLF-RAYET**

I. INTRODUCTION

The Wolf-Rayet (WR) star HD 193077 (WR138) is classified as WN + abs in the catalogue of van der Hucht *et al.* (1981). Failing to find radial velocity variations, Massey (1980) suggested that it consists of a single WR star showing absorption lines. In a subsequent study, however, Lamontagne *et al.* (1982) found radial velocity variations suggestive of a 2.3 day period in the WR spectrum, with the absorption spectrum displaying variations on much larger timescales (4.8 yrs). Hence, it was proposed that HD 193077 consists of a triple system: WN + collapsed companion in a close orbit, with an O-star in a long period orbit about the close pair. A chance line-of-sight coincidence of the O-type star with the

WR has been ruled out by Moffat *et al.* (1986) by speckle interferometry of this system. A subsequent radial velocity analysis by Lamontagne *et al.* (1982) revealed a possible orbit with a period of 1749 or 1533 days, while Annuk (1989), in a more recent analysis, refined the period to 1538 days.

On the other hand, because of the small amplitude of the 2.3 day radial velocity variations, the interpretation in terms of the presence of a collapsed companion has not been corroborated. In addition, no X-ray emission which could be attributed to a collapsed companion was detected from this source (Pollock 1987).

Robert *et al.* (1989) included HD 193077 in their study of polarization variability of the bright Cygnus stars, finding it to display small temporal variations, but with no significant periodicities.

In order to gain further insight into the nature of HD 193077, we observed this system with the IUE as part of our program to derive wind structures in WR binaries based on the variations in the emission lines (Koenigsberger and Auer 1985; Auer and Koenigsberger 1989). In this paper, we present the observed spectra and give a detailed description of the lines observable in the high dispersion IUE images of this system.

Preliminary results have been presented (Koenigsberger 1986; Koenigsberger and Auer 1987a,b) where some of the more interesting features in the *UV* spectrum of HD 193077 were pointed out. In particular, we noted the presence of "narrow" absorption components associated with the C IV and Si IV resonance lines, located at about -1250 km s^{-1} from the rest wavelengths.

Another interesting aspect of the HD 193077 system is the extraordinary width of the optical photospheric absorption lines, which if due to rotation imply $v \sin i > 500$ km s^{-1} (Massey 1980). This value is among the highest known for any OB star (Conti and Ebbets 1977). Given that the presence of "narrow absorption components" seems to be correlated with rapid stellar rotation (Prinja and Howarth 1986), the question arises as to whether the "narrow components" of C IV and Si IV arise in the WN star or in the O-star. This point is particularly intriguing.

Willis *et al.* (1986) have presented a set of identifications of the prominent lines in the high dispersion spectra of 14 WN and WC stars, a study which presents a global view of WR *UV* spectra. The intention in this paper is to present a detailed study of the spectrum of one WN. Thus, our approach has been to select all features which might be emission or absorption lines in the 1200 – 2000 A range, and attempt to assign atomic, ionic or molecular transitions to them, with the objective of gaining further information about this WN system in particular.

The paper is divided into six sections: In §II, the observations are described; in §III we give a description of the WR emission line spectrum, in §IV the absorption line spectra are presented, in §V there is a discussion of the proposed binary nature and in §VI the conclusions are presented.

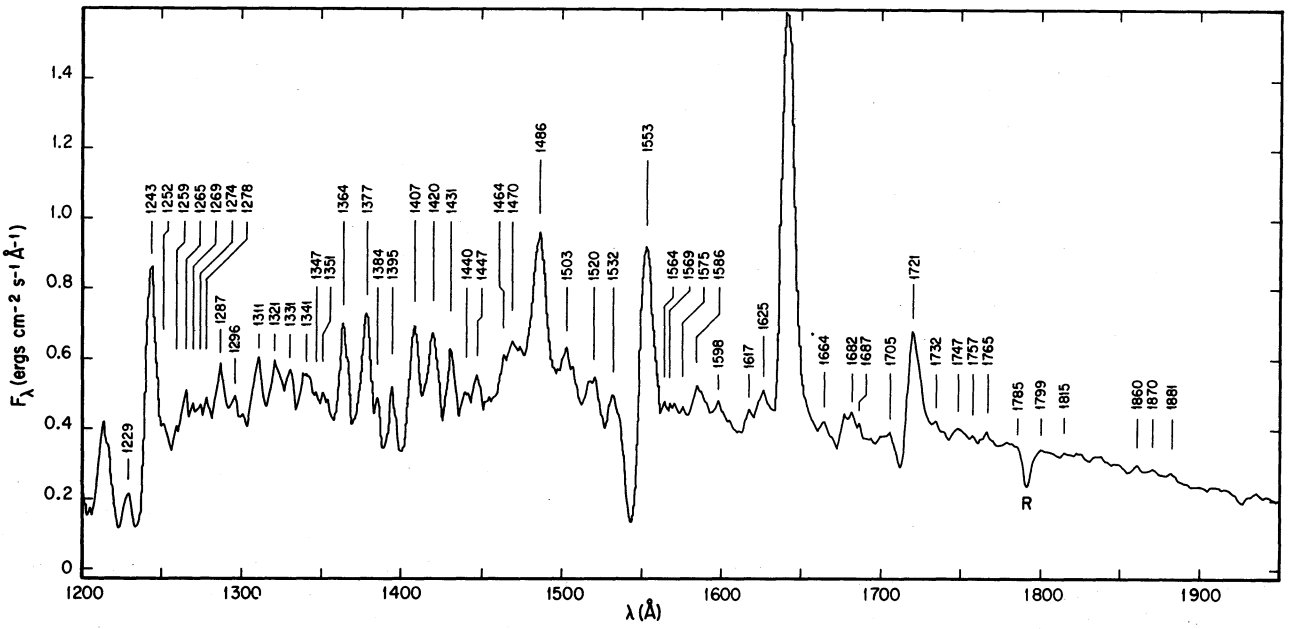

Fig. 1. The mean (over 8) low resolution IUE spectrum of HD 193077, with the wavelengths of the features listed in Tables 2 and 3. The un-dereddened flux is in units of 10^{-11} erg cm^{-2} s^{-1} A^{-1}. "R" indicates reseau.

II. OBSERVATIONS AND DATA REDUCTION

The observations were made with the IUE satellite (Boggess *et al.* 1978a,b), in both high and low dispersion by L.H. Auer in December 1981. All images were obtained with the Short Wavelength Prime (SWP) camera through the large aperture, and during the high radiation US2 shifts. An additional spectrum, SWP7000, was obtained from the NSSDC archives.

The journal of observations of HD 193077 is presented in Table 1. Altogether, we have obtained eight low dispersion and six high dispersion images over a timespan of 7 days. As noted previously Koenigsberger and Auer 1985), four of the low dispersion spectra were trailed exposures, thus requiring a correction of the exposure time by a factor of 1.07. This correction was applied.

Background radiation levels were below 75 DN's in the high dispersion and 30 DN's in the low dispersion exposures. The continuum on the high dispersion spectra was well exposed, with levels of 20 – 160 DN's at 1800 A (optimum values are 200 DN's); the emission lines were not overexposed. The mean continuum and background count levels for each exposure are listed in columns 3 and 4, respectively, of Table 1.

The FES (Fine Error Sensor) readings are listed in column 6 of Table 1. These values have been converted to the visual magnitude scale (Sonneborn *et al.* 1987) and listed in column 7 of Table 1. It is to be noted that according to Bromage *et al.* 1982) relative standard errors are very low for a case such as this where the same object was observed in identical fashion over less than 10 days and where systematic effects due to changes in temperature, procedures, etc., were expected to be very small (± 0.02 mag).

The standard extraction and reduction procedures were applied at the GSFC Regional Data Analysis Facility (RDAF). No correction for interstellar reddening has been applied. Analysis of the data has been performed with the Prime 750 computer at the Instituto de Astronomía, with codes written by J.F.Barral, and at the GSFC RDAF using the satellite link from México to the NSF internet through NCAR.

An average low dispersion spectrum was constructed by directly coadding the eight low dispersion images, and is illustrated in Figure 1. In Table 2 we list the position and absolute (un-dereddened) fluxes of all the emissions visible in the low dispersion IUE spectrum. The position corresponds to an eye-estimate of line center, which in almost all cases corresponds to maximum in flux. Each spectrum was measured independently, the average values (± standard deviation) being listed in column 2 of Table 2. The standard deviation provides an upper limit to the photometric precision (since variability may be present), and is for most of the lines below 5% (which is the quoted photometric precision of the IUE instruments).

When analyzing high dispersion spectra there are numerous sources of difficulties which must be kept in mind, especially when dealing with the spectra in detail. In particular, the echelle inter-order overlap regions may present spurious features (see c.f. Grady and Gerhart 1989) and the SWP camera artifacts resemble emission lines (Bruegeman and Crenshaw 1989). The echelle

TABLE 1

IUE OBSERVATIONS OF HD 193077

SWP Rel. Number	Date Start	Phase[a]	Count Levels Cont.	Back.	FES	MAG	Notes
15574	44936.68	0.0	140	65	2161	8.01	H
15575	44936.72	0.02	102	30	2108	8.04	L
15582	44937.70	0.44	145	74	2115	8.03	H
15583	44937.78	0.47	115	25	2091	8.05	L
15589	44937.98	0.56	100	25	2020	8.08	L
15596	44938.70	0.87	160	73	2071	8.06	H
15597	44938.78	0.90	100	26	2058	8.07	L
15603	44938.99	0.96	110	30	2045	8.07	L
15613	44940.60	0.70	120	40	2075	8.06	H
15614	44940.68	0.71	100	25	1935	8.13	L
15625	44941.62	0.14	120	45	2126	8.03	H
15626	44941.70	0.17	100	26	2193	7.99	L
15641	44942.61	0.57	125	45	2142	8.02	H
15642	44942.69	0.57	108	26	2219	7.98	L

a. Phase relative to spectrum SWP15574 and with P = 2.32 days.

TABLE 2

PRINCIPAL CONTRIBUTING IONIC SPECIES

1	2	3	4	5	6		
λ	$\langle F_\lambda \rangle$	σ	$\sigma/\langle F_\lambda \rangle$	Fe V+V I	Fe IV	This paper	Willis *et al.*
1243	8.4	0.2	2%	–	–	N V	N V
1252	4.2	0.1	2%	1252	–	Fe VI, S II	S II
1265	4.9	0.1	2%	1260	–	Fe VI, Si II, Fe II	Si II
1269	4.6	0.3	7%	1272	–	Fe VI	Si II
1278	4.7	0.2	4%	1277	–	Fe VI, Fe II, Si III	–
1287	5.7	0.2	4%	1287	–	Fe VI, N IV	N IV
1296				1296	–	Fe VI, Si III	–
1311	5.9	0.3	5%	–	–	Si III, N IV, Si III	N IV
1321	5.9	0.2	3%	1321	–	Fe V, P III	P III
1331	5.5	0.3	5%	1331	–	FeV+VI, P III, N IV	P III
1341	5.6	0.3	5%	1337	–	FeV+VI, P III, O IV	P III
1347	4.9	0.4	8%	–	–	Si II, P III	N III
1351	4.9	0.4	8%	1352	–	Fe VI, Si II	Si II
1364	6.7	0.4	6%	1362	–	Fe V, Fe VI, S III	Fe V
1377	7.2	0.3	3%	1374	–	Fe V,Fe VI,P III,O V	Fe V,P III
1384	4.8	0.3	6%	1388	–	Fe V, N III	–
1395	5.0	0.3	5%	1393	–	Si IV, Fe V	Si IV
1407	6.8	0.4	5%	1408	–	Si IV, Fe V, OIV]	Si IV
1420	6.6	0.3	4%	1420	–	Fe V, Si III	Fe V
1431	6.1	0.3	4%	1430	1426	C III, Fe V, Fe IV	Fe V
1440	5.1	0.4	7%	1441	–	Fe V, Si III	N IV
1447	5.4	0.3	5%	1447	–	Fe V, Si III	Si III
1470	6.4	0.3	5%	1465	–	Fe V, N III, Fe IV	N III
1486	9.4	0.5	5%	–	–	N IV]	N IV]
1503	6.2	0.2	4%	–	–	Si III, P III	P III
1520	5.4	0.3	6%	–	–	Fe III, Fe II	.....
1532	5.0	0.4	8%	–	1533	Fe II, P II, Fe IV	Si II
1553	9.1	0.2	2%	–	–	C IV,	C IV
1564	4.7	0.3	6%	–	1564	Fe IV	.....
1569	4.8	0.3	6%	–	–	Fe IV	.....
1575	4.9	0.2	4%	–	–	Fe IV	.....
1586	5.1	0.3	5%	–	–	Fe II,Si III,O III?	.....
1598	4.8	0.3	6%	–	–	Fe III	.....
1617	4.4	0.4	9%	–	1610	Fe IV, Fe II, C III	N V
1625	5.0	0.4	7%	–	1629	Fe IV, Fe II, C III	N V
1640	15.6	0.3	2%	–	–	He II, C III?	He II
1664	4.1	0.3	7%	–	1656	Fe IV, O III]	O III]
1682	4.6	0.4	9%	–	–	O III, Fe IV	.....
1705	3.9	0.3	7%	–	1700	Fe IV,N III,Fe IV	.....
1721	6.7	0.3	5%	–	1721	N IV, Si IV	N IV
1732	4.3	0.2	4%	–	–	Si IV	.....
1747	4.1	0.2	5%	–	–	N III], N III	N III]
1757	3.9	0.3	8%	–	–	P III, N III	.....
1765	3.9	0.2	5%	–	–	N II, O III	.....
1787	*	*	*	–	1788	Fe IV, Fe II, O III	.....
1795	*	*	*	–	–	Si IV	.....
1815	*	*	*	–	–	Fe IV	.....
1838	3.3	0.2	6%	–	–	N III, N II, Fe III	.....
1848	3.0	0.1	3%	–	–	N III, N II, Fe III	.....
1860	3.1	0.2	6%	–	–	Fe III, Fe II	N V, Al III
1870	2.8	0.1	4%	–	1872	Fe III, O III, Fe IV	.....
1881	2.8	0.1	4%	–	–	O III, Fe III	.....

Notes to Table 2: 1) Wavelength in Angstroms; 2) Mean absolute flux in units of 1. $\times 10^{-12}$ erg cm^{-2} s^{-1} A^{-1}; 3) Standard deviation; 4) Percent value of (standard deviation)/mean; 5) Wavelength of lines on synthetic Fe V + Fe VI spectrum; 6) Wavelength of lines on synthetic Fe IV spectrum.

Symbols:

..... not listed by Willis *et al.*

—— no reasonable identification found.

* unable to detect due to reseau on low dispersion spectrum.

aze, or "ripple" corrections in our data are those itomatically applied by the standard IUESIPS utines at the time of the original processing. ı additional source of emission/absorption -like tifacts, denoted "fixed pattern noise" has an timated 6% amplitude (Adelman and Leckrone 85). It is important to note that there is a large crease in the noise level at the end of the orders, ıding to possible spurious narrow features. These urces of error have been kept present constantly.

The analysis of the high dispersion data was done in three stages, each with a different representation of the same data. In the first stage, features were located and measured on an average (of the six images) spectrum kindly provided by J. Nichols-Bohlin in 1983, where special effort was dedicated to correct the wavelength scale by aligning the interstellar features and removing features due to fiducial points (reseaus). This spectrum, produced with programs written by R. Bohlin, is unsmoothed,

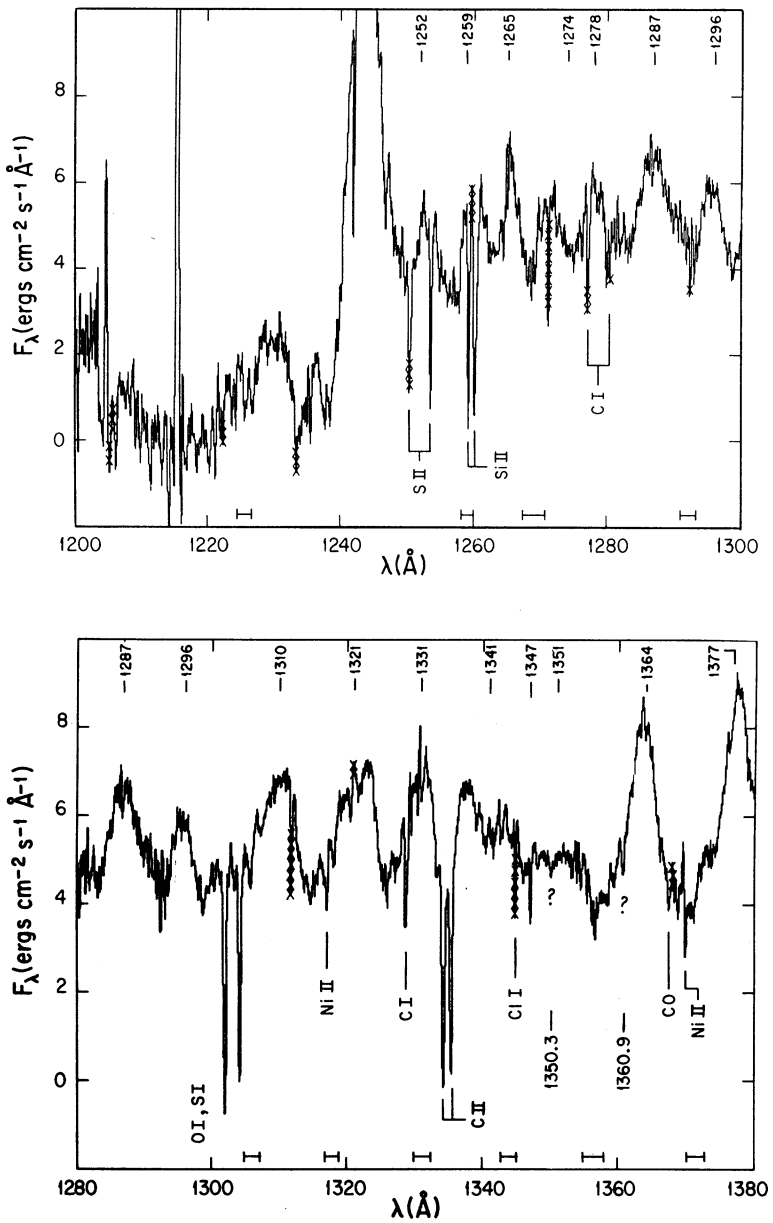

ig. 2. The mean (over 6) 11-point smoothed high resolution IUE spectrum. The wavelengths indicated above each ission correspond to those in Figure 1 and Tables 1 and 2. The more prominent interstellar features are identified. e flux scale is in the same units as in Figure 1. The wavelength ranges where the echelle inter-order overlap occurs indicated by horizontal bars below the spectrum. Bad points are indicated by a "x"

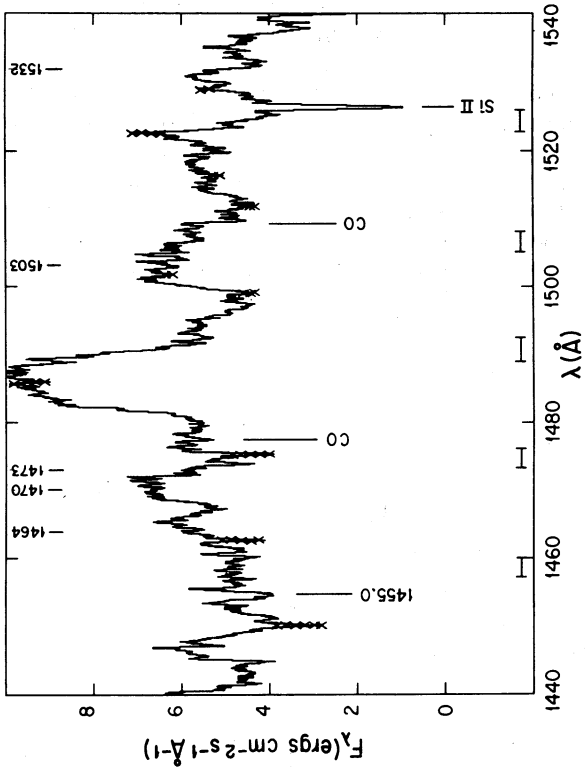

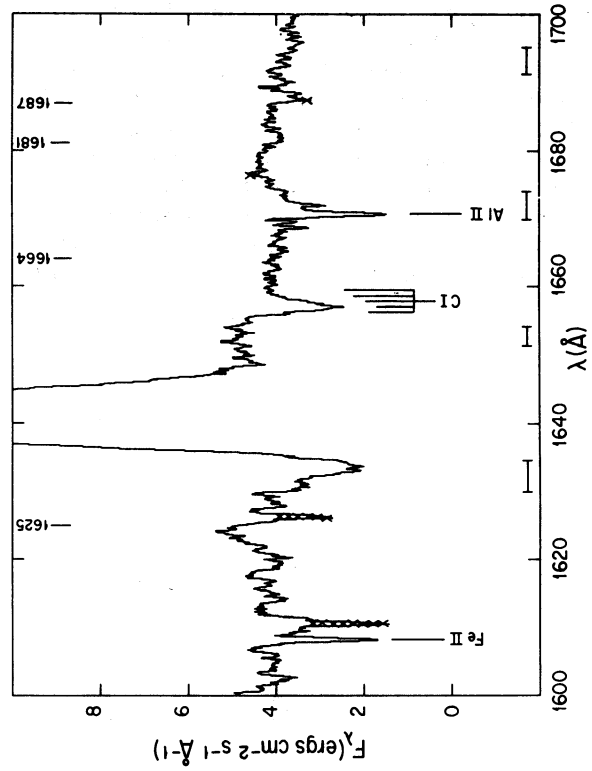

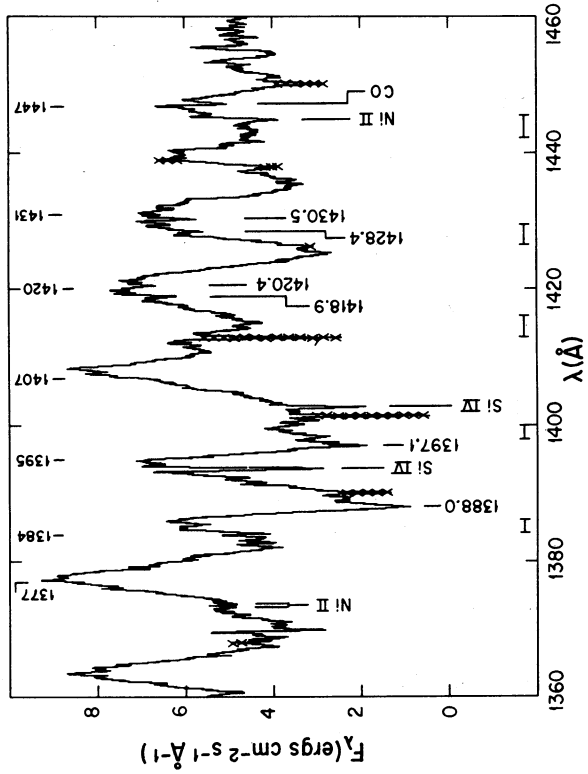

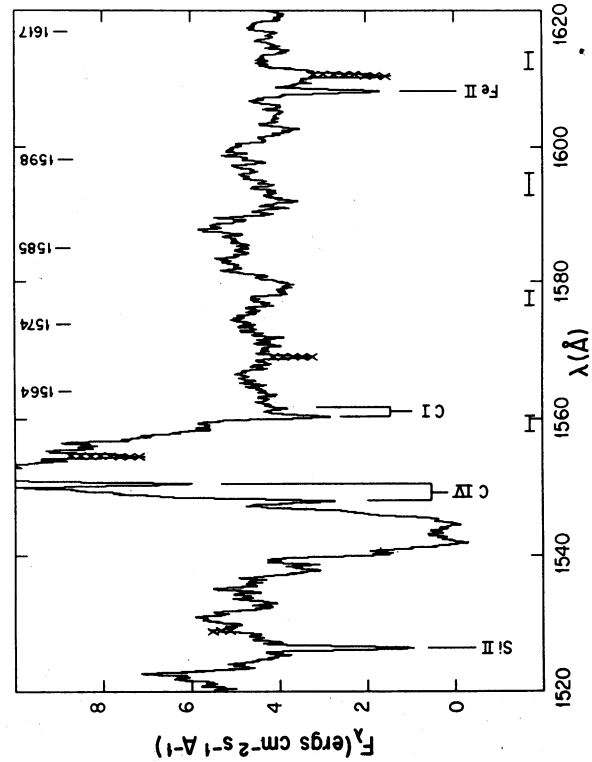

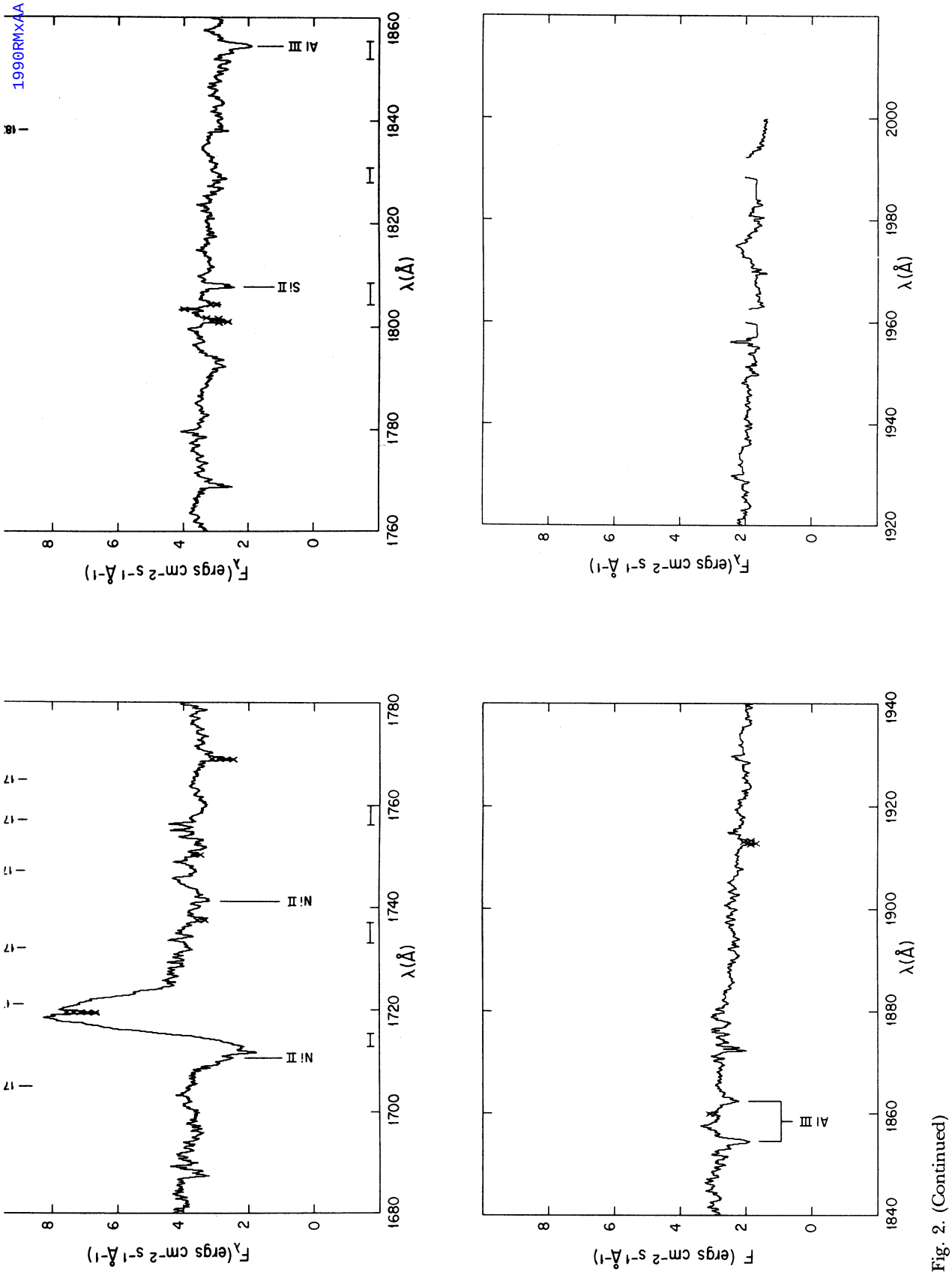

Fig. 2. (Continued)

with a sampling rate of 0.025 A per data point. This spectrum is ideal for the search and measurement of narrow, interstellar and interstellar-like features. In the second stage, an average spectrum was constructed from the six individual images in which the data were compressed into 11 point bins, resulting in spectra sampled approximately every 0.3 A. This provided a spectrum in which the measurement of WR emission lines (widths of several A) and the preliminary search for O-star photospheric absorption lines (originally expected to be 300–500 km s^{-1} wide; i.e., larger than 1.25 A at 1250 and 1.9 A at 1900 A) would be more efficient. With this sampling rate, no adjustment was required for the wavelength scale. Finally, the search for and measurement of specific photospheric absorptions was conducted on a mean of the spectra sampled approximately every 0.075 A (3-point smoothing), as well as on the unsmoothed mean spectrum.

In Figure 2 the 11-point smoothed, averag spectrum is presented in sections covering 100 . per section. The intensity scale is the same as i Figure 1, i.e., absolute, undereddened flux per un wavelength. The emission features are labeled wit the wavelength assigned from the low dispersio spectrum, and which is listed in Table 2. Th horizontal bars underneath the spectrum indicat the position of the interorder overlap region Reseaus and other points flagged in the IUESIP reduction are noted with crosses. Finally, th stronger insterstellar absorptions are labeled.

III. EMISSION LINE SPECTRUM

HD 193077 is one of the "narrow line" WN stars (Hiltner and Schild 1966), and thus, th blending of lines in the optical spectrum is not a severe as in other WN6 stars (c.f. HD 192163 HD 191765). This appears to be true in the *UV* a well, as there are numerous emission lines clearl

TABLE 3

BROAD EMISSION LINES

λ^a	$\lambda_0^b/\Delta\lambda^c$	Ident.	Multiplet	Notes
1243	1242.7	N V 1238.82	1	P
	1240.3-1249.1	N V 1242.80	1	
		N IV 1246.51	18.92	
1252	1252.2, 1254.1	Fe VI 1252.8		w(+ s.str.IS abs)
	1250.3-1255.6	S II 1250.50	1	*
		S II 1253.79		
1259	1258.6,1261.3	S II 1259.53	1	
	1257.7-1262.0	Si II 1260.42	4	
		Fe VI 1260.3		
		Fe II 1260.54	9	
		Fe VI 1260.7		
		Fe VI 1261.1		
1265	1265.4	Si II 1264.73	4	
	1263.7-1267.3	Si II 1265.73	4	
		Fe VI 1265.9		
		Fe VI 1266.1		
		Fe II 1266.69	9	
		Fe II 1267.44	9	
1274	1270.7,1271.8	N IV 1270-1273	18.75	5 lines of N IV
	1269.3-1273.7	Fe II 1272.00	9	
		Fe II 1272.64	9	
		Fe VI 1272.1		
1278	1277.8,1279.0	Fe II 1275.15	9	
	1275.5-1279.7	Fe II 1275.80	9	
		Fe VI 1276.9		
		Fe VI 1278.3		
		Fe II 1275.80	9	bl
		N II 1276.20		
		Si III 1280.30	63	
1287	1284.8,1285.8,	Fe VI 1286-1288		4 lines
	1287.5	N IV 1284.22	18.87	(P)
	1283.9-1291.1	Fe VI 1285.4		

TABLE 3 (CONTINUED)

λ^a	$\lambda_0^b/\Delta\lambda^c$	Ident.	Multiplet	Notes
1296	1294.1, 1295.1,	N IV 1296.60	18.86	
	1296.1	Fe VI 1296.9		
		Si III 1294.54	4	bl,w
	1293.6-1298.0	Si III 1296.73	4	
		Si III 1298.89	4	
	1301.	Fe VI 1299-1301		3 lines
	1299.1-(1305.4)	Fe VI 1301.8		
		Si III 1301.15	4	*bl(s.str.IS abs)
		Si III 1303.3	4	
1311	1306.5, 1310.4,	N IV 1309.56	18.55	asym.red.wing
	(1312.8)	P II 1294-1311	2	6 lines
	1305.4-1313.3	Si III 1312.6	10	
1321	1317.4, 1319.4,	N III 1324.4		
	1320.9, 1322.7	N IV 1323.98	18.81	
	1317.0-1325.0	Fe V 1323.27		
1331	1328.1, 1329.9,	N IV 1326.9	18.81	wk predicted line
	1331.5	Fe V 1330.40		bl(s. IS abs)
	1327.5-1333.6	Fe VI 1329.2		
		Fe VI 1331.2		blue wing of 1338?
1341	1337.7, 1339.4,	Fe V + Fe VI		asym.r.w.+s.IS
	1343.3	O IV 1338.61		
	1335.8-1345.5	P III 1334.9	1	
		O IV 1342.99		
		O IV 1343.51		
		P III 1344.3	1	
		P III 1344.9	1	
		Si III 1341-1343	39	
1351	1349.0, 1351.3,	Fe V + VI		
	1353.8	Si II 1348.55	7	
	1346.9-1355.7	Si II 1350.07	7	
		Si II 1353.75	7	
1364	1361.6, 1363.5,	Fe V 1359-1361		14 lines
	1364.7	Si III 1361-1369	38, 46	
	1358.6-1367.3			
-	1373.0	O V 1371.29		
	1371.4-(1373.8)	Fe V 1373.59		
		Fe V 1373.67		
		Si III 1371+1373	67	
1377	1375.5, 1377.4	Fe V 1376.34		
	1379.4, 1380.4	Fe V 1378.56		
	(1373.8)-1381.5	P III 1379.87	7	
		P III 1380.46	7	
		P III 1381.63	7	
		Si III 1375-1377	67	
1384	1384.6, 1385.7	Fe V 1385.3		
	1383.2-1386.9	N III 1387.31		
		Fe V 1385.68		
		Fe V 1387.94		
1395	1391.8, 1392.8	Fe V 1393-1395		3 lines
	1394.5	Si IV 1393.76	1	(P),s. IS abs
	1397.6, 1399.1	Fe V 1399-1404		5 lines
	1397.4-1400.5	Si IV 1402.77	1	
1407	1405.3, 1407.9	O IV] 1407.38	0.01	
	1402.9-1410.1	Fe V 1404-1410		7 lines
1420	1417.0, 1418.3,	Fe V 1415.20		
	1419.6, 1421.1	Si III 1417.2	9	
	1415.2-1424.5	Fe V 1420.46		

TABLE 3 (CONTINUED)

λ^a	$\lambda_0^b/\Delta\lambda^c$	Ident.	Multiplet	Notes
1431	1427.9,1429.5,	C III 1426-1428	11.52	
	1430.9,1432.9	Fe V 1430.57		sym.,s. abs.
	1426.3-1434.6	Fe IV 1431.43		
		Si III 1433.7	66	
1440	1437.1,1438.8,	N IV 1438.37	18.96	
	1440.0,1441.3	Fe V 1440.53		
	1436.4-1441.5	Si III] 1441.7	3.05	too red
		Si III 1436-1440	66	
1447	1446.4,1447.6	N IV 1446.11	18.85	
	1444.9-1449.1	Fe V 1446.62		
		Si III] 1447.2	3.05	
		Fe V 1448.85		
		Fe V 1449.93		
-	1452.4,1453.3	Fe V 1453-1459		
		Fe IV 1453.7		
	1451.4-1454.0			
-	1461.9,1463.7	Fe V 1462-1466		
		Fe IV 1459-1465		
	1465.2			
	1460.2-1467.1			
1470	1470.4,1473.1	Fe IV 1468-1472		
	1467.8-1473.4	N III 1470.68-A		
		Fe V 1469.00		
		N III 1471.02-A		
		N III 1471.69-A		
		Fe V 1479.47		
1486	1487.1	N IV] 1486.50	0.01	
	1480.5-1491.2	Fe III 1486.2	85	
-	1495.	Fe III 1493.6	85	
		Ni II 1500.4	7	
1503	1500.9,1505.6,	Si III 1500-1502	36	
	1508.2	Si III 1506.10	72	
	1499.6-1509.4	P III 1501.55	6	
		Si III 1501.87		
		P III 1502.77	6	
		P III 1504.72	6	
		Fe III 1505.2	85	
		Fe II 1506.5	-	g
		O V 15.07	-	
		Ni V 1501.9		
1520	1514.4,1517.8,	Fe III 1513-1525		>8 lines
	1522.1	Ni V 1519.5		
	1513.2-1524.2	Si III 1513.5	94	
		Fe II 1520.9	-	g
1532	1529.0,1530.6	P II 1532.5.	1	3 lines
	1528.3-1532.2			
1553	1551.9,1555.6,	C IV 1548.19	1	P, s abs, v.str.
	1558.8			
	1546.6-1559.8	C IV 1550.76	1	
1564	1564 1566.4	Fe IV 1563-1566		
	1563.3-1568.2			
1575	1574.3,1577.2	C III 1576.80?	12.03	
	1571.9-1577.6	Fe IV 1571-1574		
1586	1582.7,1587.7	P IV 1589.1		((P)), bl
	1580-(1584.9)	O III 1584.45		
	(1584.9)-1590.0	Fe II 1581-88	44	4 lines
		O III 1587.87		
		Si III 1588.9	59	

TABLE 3 (CONTINUED)

λ^a	$\lambda_0^b/\Delta\lambda^c$	Ident.	Multiplet	Notes
1598	1597.0, 1599.3	Fe III 1595-1601	119, 118	
	1595.0-1601.8			
		Fe III 1611.8	118	g
-	1612.7	Fe II 1611.2	-	g
	1611.4-1613.7	Fe II 1513.2	-	
1617	1617.5	Fe II 1618.47	8	(P)
	1616.7-1618.4	Al II 1616.4		
		Al II 1618.4		
1625	1621.0, 1623.7	Fe II 1621.68	8	
	1620.4-1625.3	Fe II 1625.91	8	
		C III 1620.7	11.72	
1640	---	Fe II 1631-1639	8	3 lines
	1635.4-1648.2	He II 1640.33	12	P
		He II 1640.47	12	
		C III 1645.03	11.64	
-	1652.2	Fe IV 1652.8		
	(1648.2)-1655.6			
1664	1658.5-1669.9	Fe IV 1660-1663	flat,	w, sup. abs.
		O III 1660.80		g
		Fe II 1663.22	40	
		O II 1666.1		g
		Fe IV 1675.8		
1682	1674.0-1680.7	N II 1675.75		
			27	v.broad, s.weak abs
		O III 1679.06		
1705	1701.3, 1703.1	N i II 1703.4	5	g
	1698.3-1706.2	N IV 1697-1702	18.91	3 lines
		N III 1699.32		
		N III 1699.88-P		
		N IV 1699.03	18.91	w. ?
1721	1716.4, 1718.1,	N IV 1718.55	7	P
	1719.9, 1721.6	Si IV 1722.53	10	
	1723.2			
	1714.7-1724.5			
1732	(1724.4)-(1737.7)	N III 1730.04-A		
		Si IV 1727.38	10	w. bl.with
		N I II 1748.3		
1747	1745.0, 1748.9		5	g
	1743.3-1750.9	N III] 1746.82	0.01	asym r.w.dueto s abs
		N III] 1748.61	0.01	
		N III] 1749.67	0.01	
		N III 1747.86	19	photosph.abs
		N III 1751.24	19	"
		N III 1751.75	19	"
1757	1753.0-1758.6	N III 1754.0		g
		P III 1757.7		
1765	1761.1-1768.2	N II 1763.64	14.10	v. broad; sharp
		N II 1766.08	14.10	
		O III 1760.42		
		O III 1764.48		
-	1771.7?	O III 1768.24		
		O III 1771.67		
		O III 1772.31		
		O III 1773.00		
		Fe III 1770.67		
		Fe II 1785-1787		
1787	?	O III 1784.85, Fe IV		v. broad, bl
		O III 1789.66		

TABLE 3 (CONTINUED)

λ^a	$\lambda_0^b/\Delta\lambda^c$	Ident.	Multiplet	Notes
		Fe IV 1801.5		
1795	1796.2,1799.2,	Si IV 1796.16	23	bl, s. abs.?
	1802.6,1809.3	Si IV 1796.17	23	-
	1794.5-1810.6	N III 1805	22	3 lines
1815	1814.7	Fe IV 1815.6		v.broad ?s.abs
	1812.7-1816.2			
		Fe III 1838.3		
1838	1830.3,1834.4	N III 1835.5		s. abs.,bl
	1830.2-1837.9	N II 1836.27	13.37	
		Fe III 1844-1849		
1848	1845.5	N II 1845.62		bl; sup. abs
		N III 1845.80		bl w both above
1860	1857.3,1860.0	Fe III 1855-1857	7	v wk
	1855.2-1861.1	Fe II 1857.9		
1870	1870.7,1876.1,	Fe III 1869-1877		
	1878.5	O III 1872.8		
	1869.7-1881.0	O III 1875.0		
1881	---	O III 1875.0	57	
-	1895.4-1906.3	Fe III 1895	34	multiple spikes
		Fe III 1901	95	
		Ni II 1896.1	1	g
1974	1974.0	Fe III 1976.1		
	1970.0-1978.3			

Table Headings: a) λ: Wavelength of the emission on the low dispersion spectrum. b) λ_0: Wavelength of maximum from high dispersion, 11-point smoothed mean spectrum. c) $\Delta\lambda$: Total width of the emission feature, taken at the "base" on the 11-pt smoothed, mean spectrum.

Notes: P Cyg profile; (P) probably a P Cyg profile; w weak, bl blend, not possible to separate components; b.w., r.w., blue and red wing, respectively; s superposed; str strong; g lower level of transition is ground state.

resolvable in Figure 1, particularly below 1500 A. Of the six WN systems observed in low dispersion by Koenigsberger and Auer (1985), HD 193077 has the sharpest lines. However, they are not narrow enough to escape blending effects.

The procedure followed for emission line identification can be summarized as follows: The low dispersion spectrum (Figure 1) was used to establish an initial set of lines. These lines were then searched for in the high dispersion spectrum, where the maxima were located, and additional lines were detected. This procedure was followed because the identity of an emission in the high dispersion spectrum is not always easy to determine, particularly due to the difficulty in locating an adequate continuum level. Furthermore, the superposed absorptions deform the profiles to the extent that the presence of an emission line might be questionable. The low dispersion spectrum, on the other hand, allows fi a consistent placement of a continuum througho the spectral range. In addition, we may state tha given the photometric precision established in Tab 2, all emission lines stronger than 5% of the con nuum have been located. Thus we have used tl low dispersion spectrum of Figure 1 to select tl emission features, while the high dispersion spe trum was used to locate a more precise position maximum, and, occasionally, to resolve two or mo maxima.

In Table 3 we list the estimated position maxima of all discernable emissions in the 120(2000 A range from the high dispersion spectrui Following Willis *et al.* (1986) the precision these wavelength measurements is estimated be 0.5 A, due to the problems inherent to W spectra in general (i.e., asymmetric lines, flat top

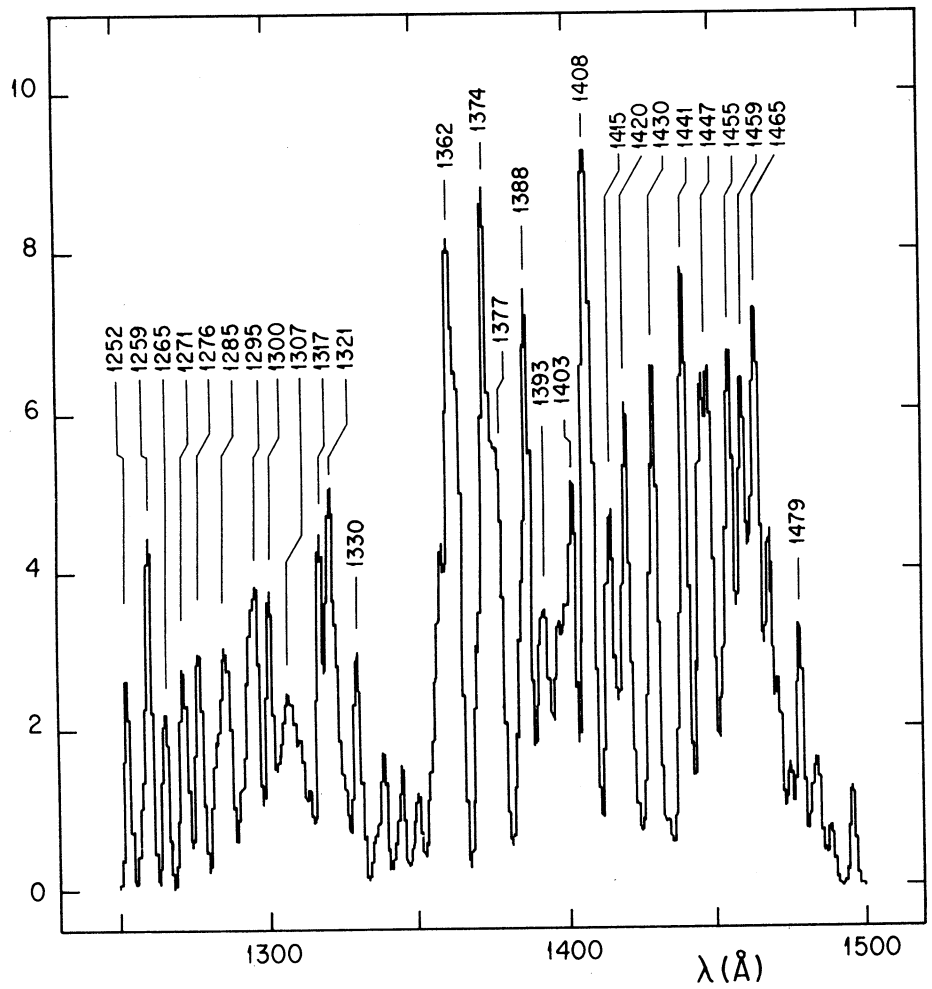

Fig. 3 Synthetic Fe V + VI spectrum constructed with the laboratory intensities of Ekberg (1975a, 1975b) with a sampling rate of 0.3 A. Wavelength positions of the blends are indicated, and are the same as listed in Table 2. The intensity scale is in arbitrary units.

superposed absorptions, etc). In column 1 we list the wavelength of the feature from the low dispersion spectrum (i.e., column 1 of Table 2); in column two we have chosen to indicate two descriptors: a) the positions of apparent maxima, separated by commas when several maxima are present, and b) the total wavelength range over which we believe the emission feature to extend. Several maxima may be present due to overlying P Cyg absorptions of neighboring lines, photospheric absorptions, or two emissions whose maxima are separated enough to be resolved. In column 3 of Table 3 we list the probable contributors to the emission, determined as described below, with their corresponding multiplet numbers in column 4, and selected comments in column 5.

Given the enormous possibilities for line identifications in this wavelength range, we first restricted our search to the following species: N III, N IV, N V, Si III, Si IV, C III, C IV, O III, O IV, O V, Fe IV, Fe V, and Fe VI, in this order, with the aid of the line lists of Kelly and Palumbo (1973), Reader *et al.* (1983), Ekberg (1975a,b) and Ekberg and Edlen (1978). It is clear from Table 3 that these species can account for almost all the emission lines listed. When a viable ID was not arrived at with these ions, the search was extended to other elements and degrees of ionization. Once a list of possible contributors to an emission line was constructed, we applied the following criteria for selection of the most likely set of contributors to a given line:

1) Abundance of the element. Reference was made to the results of element abundances by Meyer (1986), for elements not altered by nuclear proces-

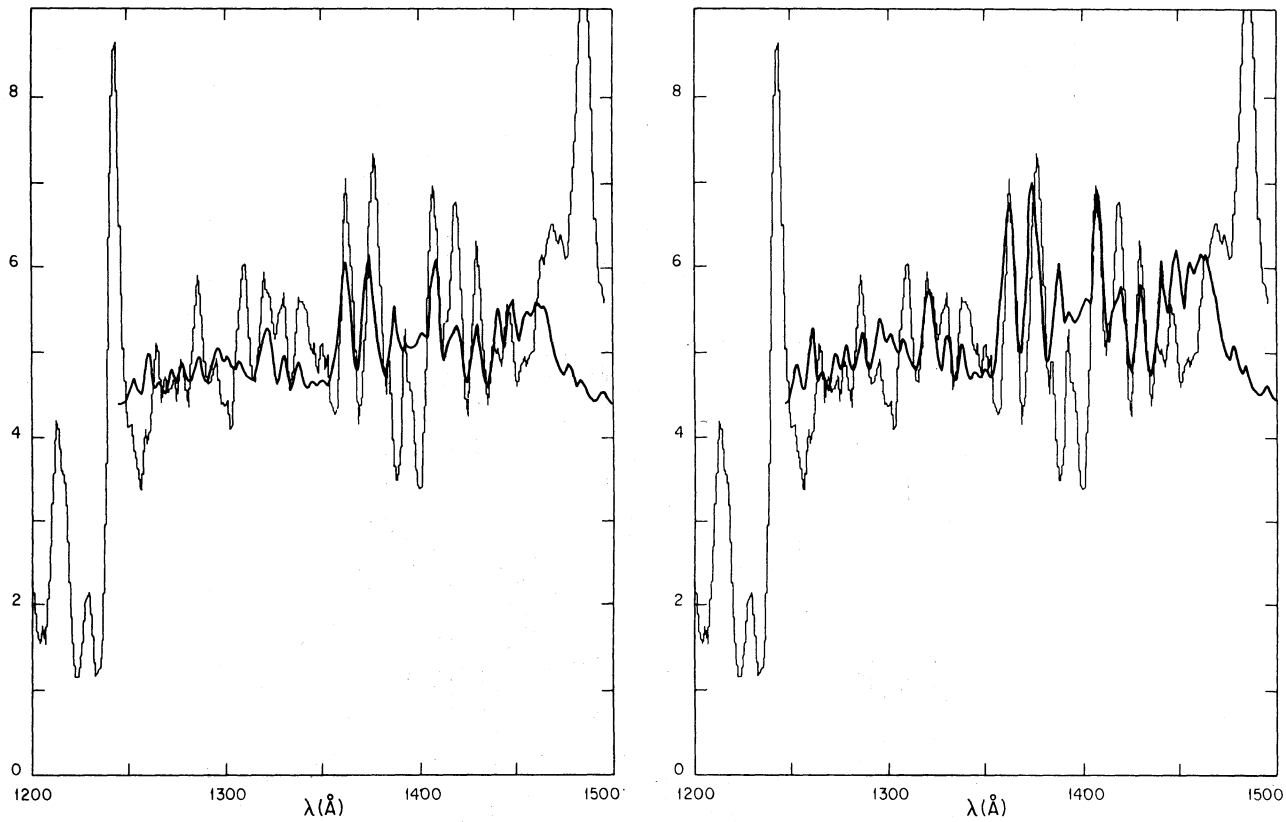

Fig. 4. The synthetic Fe V + Fe VI spectrum with a sampling rate of 1.2 A, normalized to 1460 A (Fig. 4a) and to 1377 A (Fig. 4b) is compared with the spectrum of Figure 1 (light tracing). No attempt was made to adjust the continuum of the synthetic spectrum.

sing during H-burning, and to Maeder (1983) for the expected abundances of elements in WNE stars.

2) Degree of ionization. Since HD 193077 is classified as WN6, the dominant ionization stage is that corresponding to N IV (IP = 77 eV). However, the large range in degrees of ionization present in WR winds does not allow this to be a very strong criterion.

3) Transition probability; (i.e., permitted, semi-forbidden, or forbidden).

4) Number of lines of a particular species within a small enough wavelength range.

The resultant likely identifications are presented in Table 3. The next question to be answered is whether any one ionic species is a major contributor to a given emission line. Clearly, the ideal situation is that in which a line can be associated with a transition of an abundant element, with the appropriate degree of ionization and a large transition probability, as in the case of the lines NV 1240, C IV 1550 and He II 1640. But in general this is not the case, and an accurate assessment of the relative importance of the above criteria is necessary. Because this is not a simple matter, a semi-empirical approach has been adopted, based on a very primitive spectrum synthesis model. This has been particularly useful for determining the degree to which lines of Fe IV - Fe VI contribute to the emission blends, thus allowing an assessment of the contribution by other elements as well. This spectrum sysnthesis technique has been applied previously (Koenigsberger 1988), and consists of using the tabulated laboratory wavelengths and intensities to construct an emission line spectrum, each line broadened with a Gaussian profile to widths characteristic of WR wind velocities. This is particularly useful in the case of ions such as Fe V and Fe VI whose transitions in the 1200–1500 A range lead to an enormous number of overlapping lines.

In Figure 3 we illustrate a synthetic spectrum constructed with Fe V and Fe VI lines, the intensities weighted such that there is twice as much Fe V as Fe VI, and assuming a broadening of 300 km s^{-1} (FWHM) with a wavelength sampling interval of 0.3 A. The intensity scale is in arbitrary units. In this spectrum, each "emission line" is a blend of numerous individual lines, and thus the effective wavelength does not coincide with any one

ansition. The lines are labeled with their effective avelengths. In column 5 of Table 2 we compare ıese effective wavelengths with those measured on ıe mean low dispersion spectrum of HD 193077, ıowing that from the standpoint of wavelength ɔincidence Fe V+Fe VI can indeed account for ıost of the lines below 1500 A.

In Figures 4a and 4b we present the low dispersion spectrum of HD 193077 upon which the ynthesized Fe V+ Fe VI spectrum is superposed. n Fig. 4a, the synthetic spectrum is normalized to ıe data at 1460 A, consistent with the normalization sed for the analysis of the variability in the WN+O inaries (Koenigsberger 1988). With this normaliation, only a small fraction of the equivalent widths f each line can be attributed to Fe ions. This is parcularly troublesome at 1364 A, where the only feable identification is a blend of Fe V + Fe VI (or Si II 1364), and at 1430 A, where a significant conibution by C III or Fe IV would be required to ccount for this line. As shown below, the Fe IV lies in the 1200–2000 A region are in general very eak in this system, and a strong contribution by ıe C III 1428 blend is not expected in a "normal" VN star.

If on the other hand the synthetic spectrum is ormalized to the line at 1364 (Fig. 4b), then the ɔllowing lines can be attributed almost completely to Fe: 1321, 1364 (by construction), 1377, 1407, and 1430. However, there are two problems: 1) this would imply a very small contribution by N IV 1438 and 1446; 2) the synthetic spectrum normalized in this manner predicts far more emission at 1265,1300, 1400 and 1440–1470 than observed.

With respect to the first problem, we have inspected the high resolution spectrum of HD 5980 (WN4+OI:) in the SMC, where the Fe abundance is deduced to be significantly lower than in the solar neighborhood, and the lines at 1438 and 1446 are indeed very weak, implying that the N IV contribution at these wavelengths is small. It is to be noted that, with the exception of N IV 1718 A, all N IV lines in the SWP wavelength range arise from transitions between very highly excited levels (i.e., $E_{lower} \rightarrow E_{upper} \approx 50 \rightarrow 60$ eV's, or $60 \rightarrow 70$ eV's) making them less likely to contribute significantly to the spectrum. This is true also of all the N V lines, except for N V 1240, where the transitions occur between levels with $E_{lower} \rightarrow E_{upper} \approx 75 \rightarrow 85$ eV's, and $80 \rightarrow 90$ eV's above ground level. With respect to the second problem, it must be noted that nearby each of those wavelength intervals where the synthetic spectrum predicts too much emission there is either a strong P-Cyg absorption (c.f. Si IV at 1400 A) in the data, or a possible photospheric absorption blend (c.f. Si

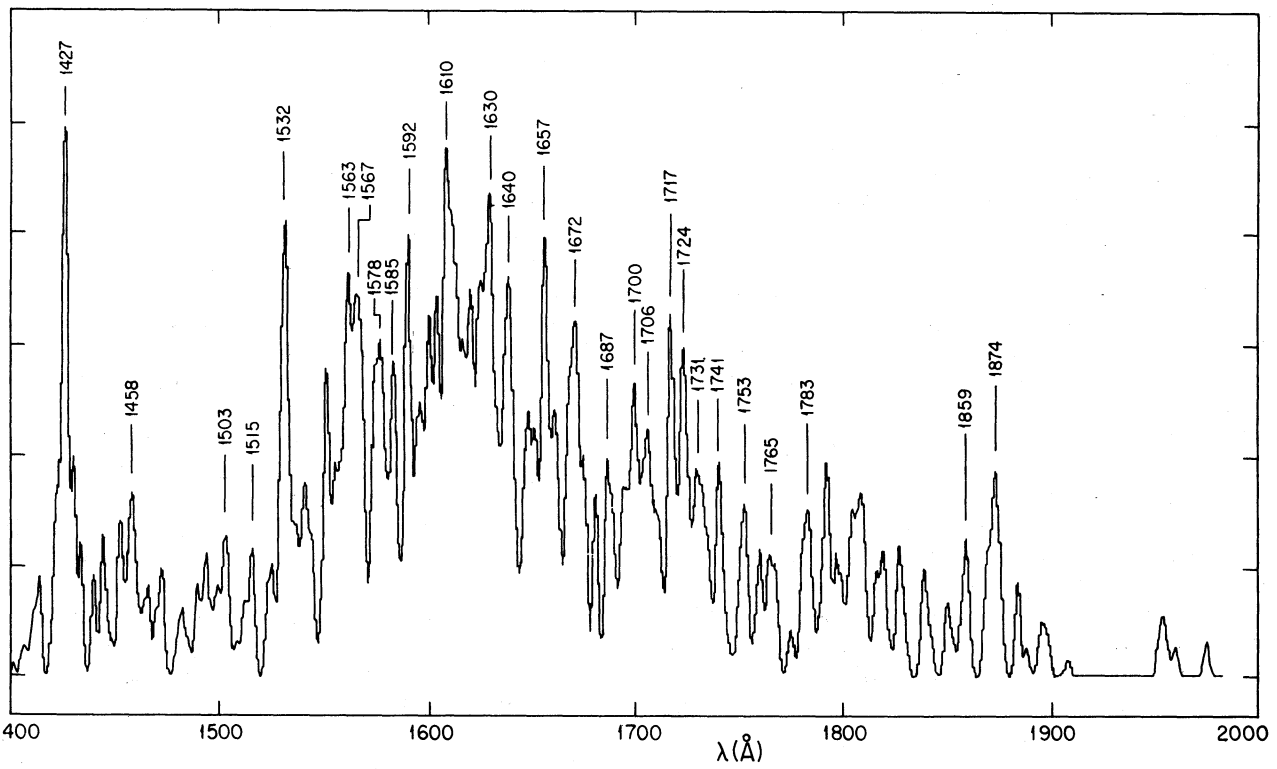

Fig. 5. Same as Figure 3, but for Fe IV, with lines taken from Ekberg and Edlen (1975).

III at 1300, Si II at 1260). Furthermore, as noted below, our method is probably underestimating the intensity of the stronger lines, which would result in an overestimate of the intensity of the weaker lines, after normalization.

In Figure 5 we present the synthetic Fe IV spectrum, constructed as the above Fe V + Fe VI spectrum, where we note that the strongest blends are found at 1610 A and 1629 A. In the spectrum of HD 193077 these lines are quite weak. Hence, we conclude that the contribution by Fe IV to the emission line spectrum is rather unimportant, although many of the weaker lines may be accounted for with this ion, especially longward of 1500 A.

It must be emphasized that the relative intensities yielded by our very crude spectrum synthesis technique can only be considered as indicative for two reasons: 1) The tabulated laboratory line intensities of Ekberg (1975a,b) are a measure of *photographic density*, but no estimate of a density to intensity calibration is given; this means that, in the case of strong lines, our method is most likely resulting in an underestimate of the intensities in the blends. 2) No radiation transfer effects are taken into account; although one might speculate that these two effects could cancel each other out, there is no question that a more precise analysis is necessary.

We thus conclude that, Fe V + Fe VI lines are major contributors, with a relatively small contribution by other ions such as Si III, P III, Fe III, Fe IV.

A similar conclusion has been reached regarding the dominance of these Fe ions in the spectra of O-subdwarfs (see Dean and Bruhweiler 1985 and references therein) and the nucleus of a PN (Feibleman and Bruhweiler 1989), although in these cases the lines are photospheric absorptions (see below).

The final list of identifications is presented in column 7 of Table 2, where, for comparison, we have listed the identifications given by Willis *et al.* (1986) for the WN6 stars in their sample. In general, our results are consistent with those of Willis et al., although there are (weaker) lines in HD 193077 which were not listed by these authors. In addition, although we favor higher ionization species for some of the lines, specifically, Fe VI lines, we disagree with the N V identifications due to the highly excited states these transitions arise from. This may not be inconsistent with the Willis *et al.* identifications for WN6 star spectra given that HD 193077 is intrinsically different from HD 192163 and HD 191765, the latter two having extraordinarily broad emission lines. Indeed, Hillier and Schmutz (1989) have suggested that a return to a version of the Hiltner and Schild (1966) classification scheme would be desirable, given the differences in the spectra of WN stars within the same subclass. However, in an analysis of the spectrum of HD 192163, Nugis and Sapar (1985) also conclude that Fe V and Fe VI dominate.

Finally, we must emphasize that we have used iron as a representative of the Fe-group. Thus, if Fe is a dominant contributor to the spectrum, all other iron peak elements must also contribute proportionately to their abundances. Hence, the identifications listed in Table 3 represent a lower limit to possible contributors.

IV. ABSORPTION LINES

a) *P-Cygni Absorption Components*

The lines which clearly have associated P-Cyg absorption components, and the corresponding "terminal" velocities are: N V 1238.8 (−1670 km s^{-1}), Si IV 1393 (−1460 km s^{-1}), Si IV 1402 (−1410 km s^{-1}), C IV 1548 (−1780 km s^{-1}), He II 1640 (−1550 km s^{-1}) and N IV 1718 (−1730 km s^{-1}). These are also clearly visible on the low dispersion spectrum. Associated with the N V, Si IV and C IV lines are narrow, sharp absorptions, which we have previously proposed to be similar to the NAC's observed in O-star's *UV* spectra. These features lie at −1250 km s^{-1} (Koenigsberger 1986).

The profile of N IV] 1486 is distorted on the short wavelength side, also indicative of a P Cyg-like absorption component associated with this line. This absorption could extend out as far as −1400 km s^{-1}.

b) *Interstellar Absorption Lines*

HD 193077 is in the Cygnus region, which is rich in interstellar material. The unsmoothed high dispersion spectrum permits the detection of weak and narrow absorptions. We have tabulated all such features which are: (1) at least two resolution elements wide and/or several times stronger than the noise level, and (2) have lower levels in the ground state, from the list of all neutral elements and low degree of ionization ions (Kelly and Palumbo 1977). In addition, we searched for lines arising in the molecular transitions tabulated by Smith (1987) and Wannier *et al.* (1982).

Our main concern with the ISM features is to discriminate between these and possible photospheric absorptions. Thus, we limit this section to the detection and identification (if possible) of ISM features.

In Table 4 the wavelength positions in the unsmoothed, mean high dispersion spectrum of all features considered to be candidate interstellar absorption lines are listed. In column 2, the estimated total width at half intensity is given. Columns 3 and 4 contain, respectively, the possible

TABLE 4

NARROW ABSORPTIONS

λ	Δ/λ	Suggested Ident.	Mult.	Velocity	Notes
1239.9	0.08	Mg II 1239.92		0	
1240.2	0.08	Mg II 1240.40		-39	
1240.4	0.08	Mg II 1240.40		0	
1243.1	0.12				
1250.5		S II 1250.5	1	0	
1253.7	0.28	S II 1253.8	1	0	
1259.4	0.28	S II 1259.5	1	0	
1260.2	*	Si II 1260.42	4	-43	
1260.5	*	Si II 1260.42	4	0	
		Fe II 1260.54	9		
1260.8	0.08	C I 1260.74	9	0	
1260.9	0.08	C I 1260.93	9	0	
1273.5	0.12	-	-		
1277.2	*	C I 1277.24	7	0	
		C I 1277.28	7	0	
1277.5	*	C I 1277.51	7	0	
		C I 1277.55	7	0	
1280.2	0.3	C I 1280.13	5	0	
		C I 1280.33	5	0	
1294.8)	0.08	Ti III 1294.7)	1	0	
1301.9	0.16	P II 1301.87	2	0	
1302.1	0.56,r	O I 1302.17	2	0	
1304.0)	-	Si II 1304.4	3	-69	
1304.3	*	Si II 1304.37	3	0	Δλ ≈ 0.4 Å
1304.4	*	P II 1304.47	2	0	
1317.2	0.16	Ni II 1317.22	10	0	IOO
1328.8	0.12	C I 1328.83	4	0	
1329.1	0.12	C I 1329.08	4	0	
		C I 1329.10	4		
		C I 1329.12	4		
1334.4	r	C II 1334.53	1	-	Δλ ≈ 0.4 Å
1335.4	*	C II 1335.66	1	(-67)	
		C II 1335.71	1	(-67)	
		C II 1335.73	2	(-67)	
1335.7	0.40	C II 1335.66	1	0	
		C II 1335.71	1	0	
		C II 1335.73	2	0	
1347.3	0.12	Cl I 1347.24	2	0	
1350.3		-	-	-	
1360.9)	0.08	Ni II 1360.96	-	0	strong
1367.6	0.16	CO 1367.62	-	0	
1370.1	0.16	Ni II 1370.14	8	0	
1373.6)	0.12	Ni II 1373.75	-	-32	
1373.9)	0.12	Ni II 1374.07	9	-44	
1388.0	0.6	Si IV 1393.76	1	-1230	
1392.5	0.20	CO 1392.53	0		
1393.6	0.08	Si IV 1393.76	1	-43	
1393.8	0.16	"	1	0	

TABLE 4 (CONTINUED)

λ	Δ/λ	Suggested Ident.	Mult.	Velocity	Notes
1396.9	0.16	Si IV 1402.77	1	-1250	
1402.5	0.08	Si IV 1402.77	1	-49	
1402.8	0.16	Si IV 1402.77	1	0	
1414.3)	0.16	Ni II 1414.30		0	
1417.6	0.08	-	-	-	
1418.9)	0.08		-		fpn?
1419.1	0.20	CO 1419.0	-	0	
1445.0)	0.16	Ni II 1445.10		0	
1447.4	0.20	CO 1447.36	-	0	
1454.9)	0.20	Ni II 1454.85	7	0	
1477.6)	0.24	CO 1477.57	-	0	
1497.0	0.20	C_3H 1497.0))	-	0	
1504.1	0.08	-			
1509.7		CO 1509.75		0	
1526.2)	r	Si II 1526.71	2	-100.	
1526.8	r	Si II 1526.71	2	0	
1533.3	0.12	Si II 1533.43	2	0	
1541.7	___	C IV 1548.20	1	-1250	minimum is saturated
1544.3	___	C IV 1550.77	1	-1250	
1548.0	0.12	C IV 1548.20	1	-39	
1548.3	0.20	C IV 1548.20	1	0	
1550.6	0.16	C IV 1550.77	1	-33	
1550.8	0.16	C IV 1548.77	1	0	
1560.2	0.08	-	-	-	
1560.4	0.24	C I 1560.31	3	0	
1560.7)	0.12	C I 1560.68	3	0	
		C I 1560.71	3	0	
1561.4)	0.08	C I 1561.44	3	0	
1608.0)	b	Fe II 1608.45	8	-80	
1608.4	0.4	Fe II 1608.45	8	0	
1620.2	0.16	-	-	-	
1625.6	0.20	Fe II 1625.9	8	-55	
1656.2	0.12	C I 1656.27	2	0	
1656.9	0.20	C I 1656.93	2	0	
		C I 1657.01	2	0	
1657.4	0.12	C I 1657.38	2	0	
1658.0	0.20	C I 1657.91	2	0	
		C I 1658.12	2	0	
1670.8	r	Al II 1670.79	2	0	
1709.6	0.08	Ni II 1709.60	4	0	
1741.2	0.20	Ni II 1741.55	5	-60.	
1741.6	0.12	Ni II 1741.55	5	0	
1748.5	0.12	Ni II 1748.28	5	+33	
1751.7	0.08	Ni II 1751.92	4	-30	
1751.9	0.08	Ni II 1751.92	4	0	
1773.9	0.1	Ni II 1773.95	3	0	

TABLE 4 (CONTINUED)

λ	Δ/λ	Suggested Ident.	Mult.	Velocity	Notes
1783.3	0.08	Ni II 1783.32		0	
1794.0	0.32	(Ca III 1794.22)		-40	broad
1807.3	0.16	S I 1807.31	2	0	
1808.0	0.33	Si II 1808.00	1	0	asym, other contr.?
1828.0?	-	-	-	-	weak
1831.6	0.30	------	-	-	
1832.0	0.30	-	-	-	-
1832.8	0.16	Al II 1832.84		0	
1845.6?	0.16	Si I 1845.52	10	0	v weak
1854.44	*	Al III 1854.72	1	-45	
1854.74	*	"		0	
1856.4?	0.08	Fe III 1856.69	63	-48	strongest of multiplet
1862.5	0.16 *	Al III 1862.79	1	-44	
1862.9	0.20 *	"	1	0	
1885.7?	0.18	Ni II 1886.04	23	-48	

Notes: * Lines are blended, though minima are resolved; width refers to total half width of blend; λ line center or position of minimum if multiple; r Russeau or bad point make measurement unreliable; error ± 20 km s^{-1} at 1300 A (i.e., ± 0.1 A uncertainty); fpn fixed patter noise; I00 near inter-order overlap region.

identification and the multiplet number of the transition, when available, and column 5 contains the approximate velocity displacement, with respect to the laboratory wavelength of the transition.

All the interstellar lines usually detected (see for example, Willis *et al.* 1986; Dean and Bruhweiler 1985) are present. Additional lines present in our data include almost all members of multiplets 2 through 9 of C I, ground-state transitions of Ni II, Mg II and the (n,0) rotational transitions of CO. All these are approximately at their laboratory rest wavelengths. In addition, as shown in Table 4, various lines have components at about −45 km s^{-1}, with respect to the undisplaced line. This occurs exclusively with the higher ionization species. St. Louis *et al.* (1988) have recently examined the interstellar lines which are present in the spectra of several stars located near HD 193077. They find high velocity components to be a common feature, thus concluding that there is a large scale shell along the line of sight to these stars. The nature and origin of this possible large "bubble" is an interesting question which requires further study.

c) *Photospheric Absorptions*

(i) Identifications

There are regions in the high dispersion spectrum of HD 193077 in which the presence of broad absorption features is suggested. Given the complicated nature of the spectrum, the identification of photospheric absorptions requires in many cases a great deal of imagination.

Two procedures were followed: 1) From an inspection of the Atlas by Walborn, Nichols-Bolin, and Panek (1985), a list of the strongest photospheric absorptions present in O3-BO stars was constructed, and these lines were specifically searched for. This procedure was useful only in part, since all the strongest lines (Si IV, C IV, He II, N IV) coincide with broad WR P-Cyg features, making the detection of broad, overlying absorptions almost impossible. Other very prominent lines in the spectra of OB stars, such as O IV 1338, 1343 were not obvious either. 2) An inspection of two SWP spectra of V444 Cyg (WN5+O6), corresponding to two different orbital phases (SWP 26041, ϕ = 0.46; SWP

26000, $\phi = 0.76$) suggested that a search for distorted emission lines and shallow dips is more appropriate in this type of system. We thus searched for such features on the 3-pt smoothed mean spectrum of HD 193077, since the improved signal to noise ratio is expected to enhance the photospheric absorption lines of a companion whose orbital motion during the 7 observation days is presumably negligible. These features do indeed appear in the spectrum, although defining a line center is practically impossible. Hence, we chose to record the wavelength range over which we consider the feature to extend.

Once the list of candidate photospheric absorptions was constructed, we measured the lines in the spectrum of 10 Lac (O9V; SWP 17394) which lie at similar wavelengths, to facilitate the identification procedure. Furthermore, each individual spectrum was inspected. The higher noise levels make detection of the broad and shallow features very difficult. However, the lines such as 1420.5 and 1430.4, which are superposed on an emission and which are relatively narrow were easily detected, although not on all spectra.

In Table 5, the first column contains the wavelength range over which we estimate the feature to be present, with the corresponding velocity range in column 2. In column 3 is the position of pho-

TABLE 5

PHOTOSPHERIC ABSORPTIONS IN THE SPECTRUM OF HD 193077[a]

Wave	DV	10 Lac	HD 46202	Other	
1225.5-1227.4	450	1225.5	S II 1226.7	N IV 1225.7	1
1228.9-1230.7	400	1227.3	S II 1227.4		
	-	1229.8	-	Fe VI 1229.9	
1246.5-1247.0	100	1247.7	C III 1247.8		
? -1260.9	-	1261.2		Fe VI 1261.1	
1272.5-1276.0	-			Fe II 1272-76	
1276.9-1277.5	150	1276.9		Fe VI 1276.9	
1264.4-1264.7	70	-		Ni V 1264.5	
1264.3-1265.3	250			Si II 1264.7?	
1286.1-1286.9)	200)	1287.0		Fe V 1287.1	
1302.6	-	1302.7	-	-	
1303.0-1303.8)	-	1303.2	Si III 1303.2		
1305.3-1306.0)	150)	1305.9			
1306.8-1307.9	250	1307.3		Fe V 1307.4	
1307.0-1310.4	800				Si II 1309.3
1312.5-1316.0	800				Si III 1312.6
1317.7-1318.1	90	1317.9		Fe V 1317.9	
1320.2-1320.7	100	1320.4		Fe V 1320.4	
1321.3-1322.4	250	1321.3	Fe V 1321.3+21.5		
		1322.2	-		
1323.9-1326.9	700	-		N IV 1324.0-26.9	
1323.9-1324.2	70	1323.8		N IV 1324.0	
1333.2-1333.5	-	-	-	-	
1332.5-1337.0	<1600>	-	-	-	C II 1334.5+35.7
1338.7-1339.1)	90)	1338.6	O IV 1338.6		
1340.0-1340.8	100)	1340.7)	-	-	
1341.1-1342.2)	250)		-		
1342.6-1343.1)	100	1343.1	O IV 1343.0		
1356.0-1357.1	250	1356.0		Ni IV 1356.1	
		1356.9	Ni IV 1357.1		
1357.9-1358.8)	200)	-			P Cyg?
1358.1-1358.7	150	1359.0		Fe V 1359.0	
1360.4-1360.9	100	1361.3		Fe V 1361.3+61.4	

TABLE 5 (CONTINUED)

Wave	DV	10 Lac	HD 46202	Other
1363.8-1364.0		-		Fe V 1363.6)
		1365.0		Fe V 1365.1
1370.7-1371.6)	200	1371.2		O IV 1371.3
1373.1-1374.5	300	1373.6	Fe V 1373.6+73.7	
1376.2-1376.8	150	1376.2	Fe V 1376.3+76.4	
1384.9-1385.7	150	1385.3)	Fe V 1384.7+85.7	
1387.5-1388.4	200	1388.0		Fe V 1388.2 2
1404.5-1405.3)	150	1405.8		
1414.1-1414.4	50	1414.6		Fe V 1414.8
1418.9-1419.1	40	1419.2		O V 1419.0)
1420.2-1420.9	150	1420.1	Fe V 1420.1-20.6	
1425.0-1425.4	80	1426.0	Fe IV 1425.5	Fe V 1425.1 IOO
1428.2-1428.5	60	1428.8)	CIII 1428.2+29.0	Fe V 1428.1
1430.0-1430.5	100	1430.4	Ni IV 1430.4	Fe V 1430.3+30.6
			Fe IV 1431.4	
1437.5-1438.1	100	1437.5))	-	-
1444.7-1445.1	80	1444.2))	-	-
1447.0-1447.5	100	-	-	Si III1447.2?
1448.6-1449.1)	100			Fe V 1448.8
1451.1-1451.7)	100	1452.2		Fe V 1451.1
1454.2-1455.3	250	1454.5		Fe V 1454.2+54.7 Ni IV 1454.8?
1459.8-1461.4	350	1460.4	Fe V 1459.8	Fe V 1460.7+61.1
1464.2-1464.4	50	1464.6	Fe IV+V 1464.7	
1465.7-1468.4	550	1466.5		Fe V 1466.6
				Ni II 1467.3+67.8 or P Cyg
1473.5-1474.1	60	1473.0+1472.5		Fe IV 1473.2
1474.8-1475.6	150	-		Fe V 1475.6
1477.3-1477.6	50	1477.5		Fe V 1477.8
1511.5-1513.4	400	1511.0	Ni IV 1512.7	Mn V 1511.1
1519.5-1521.4	350	1520.5	Ni IV 1520.6	Mn V 1519.6+19.8
1524.2-1528.7	900	1525.1		Ni IV 1525.3
		1526.2		Fe IV 1526.1+26.6
		1527.6	Ni IV 1527.7	
1529.7-1530.1	100	1530.0		Fe IV 1530.2
1532.0-1533.7	350	1532.5	Mn V 1533.1	Fe IV 1532.6+32.9
			Fe IV 1533.3+33.9	
1537.2-1538.9	400	-	Ni IV 1537.2+38.9	
			Fe IV 1538.3	
1583.6-1587.2	700	1584.0	-	Fe IV blend
		1584.9		Fe IV 1484.9
1597.3-1598.0	150	1597.9		Fe IV 1598.0
1600.6- ?	-	1600.3	Fe IV 1600.5+00.6	
? -1603.0	-	1601.1		Cr V 1603.2:
1603.6-1606.3	500	1604.6	Fe IV 1603.7	
		1605.6	Fe IV 1605.7+06.0	
1609.9-1611.5	350	1610.4	Fe IV 1609.8+10.5+11.2	
				Cr V 1611.3
1618.6-1620.6)	350)	1620.8	Fe IV 1619.0+20.9	
1621.6-1622.0)	90)	-	Fe IV 1621.6	
1625.1-1626.8	300	1626.6	Fe IV 1626.3	Fe V 1625.3

TABLE 5 (CONTINUED)

Wave	DV	10 Lac	HD 46202	Other	
1630.0-1631.9)	350	1631.2))	Fe IV 1631.1		
1655.7-1658.1	450	1655.8-1658.4		Cr V1655.6	
1680.4-1682.6	300	1681.1	Fe IV 1681.3		
		1681.7	Fe IV 1681.9		
1687.3-1688.4	250	1686.5	-	N IV 1687.6	Fe IV 1688.4 ?
		1687.5		N IV 1687.8	
		1688.4		N IV 1688.1	
1689.6-1690.9)	250	1690.2	Fe IV 1690.3		
1692.1-1700.5	1500	1694.4	Fe IV 1695.0	v.shallow	
		1697.4	Fe IV 1697.5		
		1698.8	Fe IV 1698.9		
		1700.2	Fe IV 1700.4	N IV 1699.0	
		1700.7	Fe IV 1700.8		
1698.1-1701.0	350	within above			
1696.9-1797.2)	50	"		N IV 1696.9	
1703.7-1707.2	600	1704.0	Fe IV 1704.2		
		1704.8	Fe IV 1704.9	Cr V 1705.6+06.0	
		1707.1		Fe IV 1707.2	UWCMa
1716.1-1717.5)	250)	1718.0	Fe IV 1717.9		P Cyg
1722.0-1723.1)	200)	1722.5	Si IV 1722.5		
			Fe IV 1722.7		
1724.5-1725.4	150	1724.0	Fe IV 1724.0+24.6		
		1725.4	Fe IV 1725.6		
1731.4-1733.1	300	1732.8	Fe IV 1732.9		
1737.1-1738.0	150	1738.6	-	-	
1739.6-1740.4	150	1740.0	-		
1741.0-1742.0	150	1742.0	-	Ni II 1741.6	
1745.8-1748.6	500	1746.9	-		4
		1747.7	N III 1747.9		
1751.0-1753.8	500	1751.1	N III 1751.2		
		1751.5	N III 1751.7		
		1752.8	-		
1757.8-1761.7	650	1758.4	Cr IV 1758.5		
		1760.3		Ni III 1760.6	
		1761.0		Fe IV 1761.1	
1762.4-1763.4	150	1762.8	-		
1788.1-1795.1	1150	1788.4)	-	Ni II 1788.5?	
1803.8-1805.0	200	1804.3	N III 1804.3	Ni II 1804.5	Sharp core in flagged
1807.2-1808.3	200	1807.6	-		
1810.5-1813.5)	500)	1811.1		V V 1811.4	
		1812.2	Cr IV 1812.4		
1817.1-1822.2	850	1817.	-		
		1819.1	Cr IV 1819.2		
		1820.0		Fe IV 1820.0	UWCMa
1837.7-1844.6	1100	1837.4		Cr IV 1837.4	
		1840.0	Fe IV 1840.2		
		1841.2			
		1842.9			
1850.5-1851.7	200	1851.9	Fe IV 1850.6		
1858.3-1859.6)	200)	1860.4	Fe IV 1860.4		
1884.4-1896.0)	1850	1885.0	Si III 1892.0		
			N III 1885.25		
1921.3-1926.1)	750	1922.4	-	-	C III 1923
		1926.1	-	-	

a. Measured on 3-pt smoothed mean constructed from 6 unsmoothed individual spectra.

tospheric absorptions measured in 10 Lac. Column 4 contains the identifications, taken from Dean and Bruhweiler for the O9V star HD46202, while in column 5 we list the identifications given by Dean and Bruhweiler for two O subdwarfs and/or by Drechsel *et al.* (1981) for UW C Ma. Additional possible identifications are listed in Column 6, taken from Kelly and Palumbo (1973) and Striganov and Svetitskii (1968).

The first point to note is the presence of narrow, high ionization lines, specifically, Fe V. The full widths of these lines are on the average 250 km s^{-1}. Also present with relatively good likelyhood are lines of Fe IV, Ni IV. Lines of N IV and N III are definitely present. In the spectrum SWP 7000, a narrow feature at 1339.1 A is clearly present, with FWCI = 0.3 A, attributable to O IV. In addition, the shape of the distorted emission lines is strongly suggestive of the presence of broad superposed absorption lines (difficult to distinguish from possible not-fully-developed P-Cyg absorptions, except for the feasible identifications) due to ions such as Si II, and possibly C II. Thus, the spectrum of HD 193077 has features which might be indicative of the presence of a hot subdwarf, such as those studied by Dean and Bruhweiler.

Photospheric absorption lines of Fe V have been detected in at least 3 other WR-type stars: HD 93162 (WN7) and HD 193793 (WC7) by Fitzpatrick (1982) and HD 45166 by Willis and Stickland (1987).

It is interesting to note that a combination of high *(UV)* and low (visual)– degree of ionization photospheric lines has also been found in the peculiar system HD 45166 (Willis and Stickland 1983; Willis *et al.* 1989), and this has led to the conclusion that the system consists of a B8V star in orbit about a possible O-type subdwarf. However, despite the major line variability (Willis *et al.* 1989) observed in this system, no orbital period has been detected.

In Table 6 we list those lines which we consider

TABLE 6

PHOTOSPHERIC LINES BY IONIC SPECIES

Ionic Species		FWCI[a]	RV[a]	Ionic Species		FWCI[a]	RV[a]
N IV	1225.7	450	- 50		1459.8 + 61.1	350	-
	1324.0	70	0		1466.6	550	+100
	1687.6-88.1	250	0		1475.6	150	- 80
N III	1747.9	500	-120	Fe IV	1473.2	60	+120
	1751.2+1.7	500	0		1532.6 + 32.9	350	0
	1804.3	200	+ 20		1603.7 + 06.0	500	0
					1609.8 + 11.2	350	0
O V	1371.3	200	0		1619.0 + 20.9	350)	- 50
	1419.0	80			1621.6	70)	+ 30
					1626.3	300	0
O IV	1338.6	90)	+ 70		1631.1	350	- 20
	1343.0	100)	- 30		1681.3 + 81.9	550	- 20
					1690.3	250	- 20
Si III	1312.6	800	+360.		1704.2 - 07.3	600	- 60
					1722.7 (+SiIV)	200)	- 20
Si II	1309.3	780	-140		1724.0 + 24.6	150	+120
					1732.9	300	-120
Fe VI	1276.9	150	+ 70		1850.6	200	+100
	1285.4	70	- 50		1860.4	200)	-240
Fe V	1287.1	200)	-140	Fe III	1583.2	700	-
	1307.4	250	- 25		1819.5 + 20.5	850	0
	1317.9	90	0				
	1320.4	100	+ 25	Ni V	1264.5	70	0
	1321.3 + 21.5	250	+ 90				
	1358.6	150	- 40	Ni IV	1356.1 + 57.1	250	+ 70
	1363.6	40)	+ 70		1512.7	400	- 80
	1373.6 + 73.7	300	+ 20		1520.6	350	- 40
	1425.1	80	+ 20		1537.2 + 38.9	400	-
	1428.1	60	+ 60		(+ Fe IV 1538.3)		
	1430.6	100	0				
	1437.5	100	+ 60	H I (H 11) *		1500.	-
	1451.1	100)	+ 40				
	1454.2 + 54.7	250	+ 40	He I 3820 *		1000.	-

* From Figure 1 of Massey (1980). a. FWCI and RV in units of km s^{-1}.

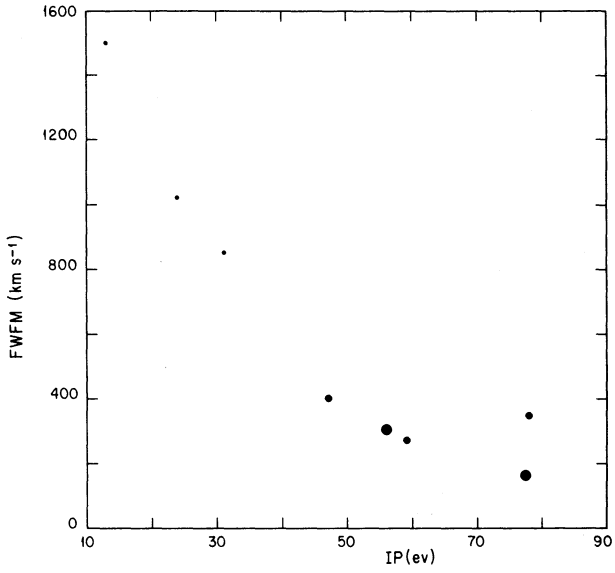

Fig. 6. Correlation of full width at continuum intensity (FWCI), measured in km s^{-1}, with the ionization potential of the observed photospheric lines.

most likely to be present and which suffer from minimum blending effects, ordered according to element and degree of ionization. In column 1 is the ionic species with the laboratory wavelength, in column 2 is the total width of the feature (in km s^{-1}), and in column 3 is the velocity displacement, with respect to the laboratory wavelength, of the "center" of the feature, defined simply as the middle of the wavelength range given in column 1 of Table 5. Also included are the average values for each ion, and values of FWCI for lines of H and He, estimated from Figure 1 of Massey (1980). In this table a tendency for a progression in line widths as a function of ionization potential is present, and is illustrated in Figure 6.

It is worth noting that, in Massey's analysis of the line-profile broadening, he found $v \sin i$(H) = 550 km s^{-1} while $v \sin i$(He I) = 475 km s^{-1}, although he did not attribute significance to this difference.

There are two main conclusions to be derived from the photospheric spectrum:

1) The absorption spectrum in the *UV* consists of narrow, high-degree-of-ionization lines (Fe V, N IV, Fe IV, Ni IV, O IV?) as well as broad lower ionization lines (Fe III, N III, Si III, C II, Si II).

2) When optical H and He lines are included, there is a strong correlation between the FWCI of the lines and their ionization potential.

ii) Variability?

The great difficulty we have had in measuring the photospheric lines may be due, in part, to variability. As mentioned above, all lines are not present on all six spectra. It is difficult at this time, however, to conclude that the spectrum is definitely variable. However, there is a trend over the 7 days of observations for a systematic decrease in visibility of the lines at 1428 A and 1430 A and an increase in the lines at 1419 and 1420 A. This is illustrated in Figure 2, in Koenigsberger and Auer (1987a). Assuming our identifications are correct for these lines, then there is indication of a changing degree of ionization over the 7 days.

In addition to the above, it must be noted that, for example, the Fe IV 1732 line is clearly in absorption in SWP 15574 and 15582 (W_λ = 225 A) but overwhelmed by apparent emission in the other spectra.

V. DISCUSSION

The emission line *UV* spectrum of HD 193077 is dominated by high ionization species, primarily Fe V and Fe VI blends, in addition to the usual strong lines observed in all WN stars in this wavelength range. The photospheric spectrum contains both high and low degree of ionization lines, with an anti-correlation between the ionization potential and the FWCI, which is fully consistent with the presence of a rapidly rotating hot star (Hutchings 1976; Sonneborn and Collins 1977; Sonneborn 1982).

The fundamental question here is: Do both spectra originate in the same star, or is this a binary system? Massey (1980) noted that the equivalent widths of the optical photospheric lines were very similar to those of O-stars in general (both for massive O-stars and nuclei of planetary nebulae); he states *"Taking into account the continuum of the WR (assuming it to be a binary) means that the absorption lines would be unusually strong"*; and thus concludes *"either the OB star's continuum dominates at these wavelengths, or there is only one star present with normal equivalent widths"*. However, if the O-star dominates, then the WR star is disturbingly fainter than expected for its subclass. The *UV* (low resolution) emission-line spectrum of HD 193077 is almost identical to that of the binary V444 Cyg at orbital phase 0.75; i.e., when no eclipse/scattering effects are present. The equivalent widths of the emission (We) and the absorption (Wa) components of N IV 1718 are slighly larger than observed in V444 Cyg, but do lie within the range of values measured for other binary systems (HD 211853, WN6 + O+O?; and HD 94546 (WN4 + O6V:) which we have studied previously (Koenigsberger 1983; Koenigsberger and Auer 1985).

In Table 7 the equivalent widths of the few photospheric absorption lines which could be measured with certain reliability are listed, and compared with those measured in 10 Lac (O9V), and V444 Cyg

TABLE 7

COMPARISON OF PHOTOSPHERIC LINES

Feature	Equivalent Widths (m A) HD 193077	V444 Cyg	10 Lac
Fe V 1420	20	30	430
Fe V 1430	40	60	460
FeIV+V1464	30	20	170
Fe IV 1473	90	-	(200)
Fe V 1477	30	40	>100
Fe IV 1681	170	120	450
N IV 1687	200	100	450
N III 1747	160	170	300
N III 1751	20	60	400
N III 1804	50*	-	240

* Flagged pixels removed.

(WN5 + O6V:). The measurements of the features in the WR spectra were made after "rectifying" the spectrum; i.e., the spectra were smoothed using 45 points, and then the ratio of the unsmoothed to the smoothed spectrum was constructed. This yields a fairly constant "continuum" level at a value of unity. If we assume the absorption features to arise in the companion O-stars, we can estimate the relative continuum fluxes of the two members within a binary system with $F_1/F_2 = (W_2/W_{obs}) - 1$, where W_2 is the equivalent width of the feature in the O-star and W_{obs} is the measured equivalent width. F_2 is the continuum level in the O-star. In Figure 7 we illustrate the dependence of the observed absorption equivalent width arising in a star which is a member of a binary system on F_1/F_2. Taking the N IV 1687 blend as the most reliable line, and using the value of $W_2 = 450$ mA from 10 Lac results in $F_{WR}(\text{V444})/F_{06} = 4.5$, $F_{WR}(\text{HD 193077})/F_0$ = 2.2. This would seem to imply that the O-star continuum in HD 193077 is indeed more dominant than that in the O-star in V444 Cyg, even in the *UV*, but in any case, the conclusion would seem to be that HD 193077 is a binary system. There is, however, one serious flaw in the above arguments. There is little question that the photospheric absorption line spectrum arises in a rotating star. This means that the higher ionization lines, such as we have considered here, originate primarily in the polar regions, (Hutchings 1976) and perhaps not at all in the equatorial regions of this rotating star. The polar regions of a star are a portion of the *limb* of a star, and thus, the (pure absorption) lines observed to arise in these regions will be weaker than the lines which would be observed to arise from the entire stellar disk of a non-rotating star of similar temperature and gravity.

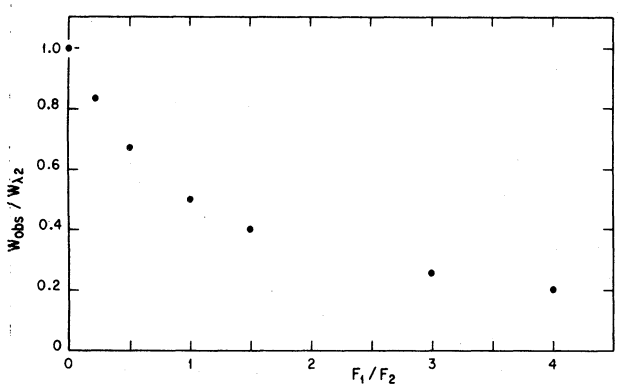

Fig. 7. Dependence of the observed equivalent width of a line (assumed to arise in only one star) as a function of the continuum luminosity ratio of the members of the binary system. W_{tot} is the measured width. In this case, F_2 represents the presumed O-star companion.

Let us consider the equivalent width which we would observe if the line-forming region were constrained to only a fraction of the stellar surface between the equator and the pole (limb). Assuming a pure scattering continuum ($\rho = 1$), the emergent intensities in the line and in the continuum at the surface as given by Mihalas (1978) reduce to:

$$I_\nu(0,\mu) = (a + p_\nu\mu) + \frac{(p_\nu - \sqrt{3}a)\left(1 - \frac{\epsilon\beta_\nu}{1+\beta_\nu}\right)}{\sqrt{3}\left(1 + \sqrt{\frac{\epsilon\beta_\nu}{1+\beta_\nu}}\right)\left(1 + \sqrt{\frac{3\epsilon\beta_\nu}{1+\beta_\nu}}\mu\right)} \quad (1)$$

$$I_c(0,\mu) = b(\mu + 1/\sqrt{3}) \quad .$$

Here, μ is the cosine of the angle between the emergent ray and the normal to the stellar surface, and, $\beta_\nu = \chi_l\phi/\sigma_e$, $p_\nu = \frac{b}{1+\beta_\nu}$ and a, b are the coefficients of a linear expansion of the Planck function, $B_\nu(T(\tau))$:

$$B_\nu = a + b\tau \quad .$$

The residual intensity is defined as

$$R_\nu = H_\nu(0)/H_c(0) \quad ,$$

with

$$H_\nu(0) = \int I_\nu(0,\mu)\mu d\mu$$

$$H_c(0) = \int I_c(0,\mu)\mu d\mu$$

Substituting from (1), and integrating over μ from 0 (the pole or limb) to μ_c:

$$\int_0^{\mu_c} I_\nu(0,\mu)\mu d\mu = \frac{p_\nu}{3}\mu_c^3 + \frac{a}{2}\mu_c^2 +$$

$$+ \alpha\left[\frac{\mu_c}{\sqrt{3\lambda_\nu}} - \frac{1}{3\lambda_\nu}\log\left(\sqrt{3\lambda_\nu}\mu_c + 1\right)\right] , \qquad (2)$$

$$\int_0^{\mu_c} I_\nu(0,\mu)\mu d\mu = \frac{b}{3}\mu_c^3 + \frac{b}{2\sqrt{3}}\mu_c^2 \quad ;$$

where

$$\alpha = \frac{(p_\nu - \sqrt{3}a)\left(1 - \frac{\epsilon\beta_\nu}{1+\beta_\nu}\right)}{\sqrt{3}\left(1 + \sqrt{\frac{\epsilon\beta_\nu}{1+\beta_\nu}}\right)} \quad .$$

If one takes the limit for a very strong line, and assumes a pure absorption line ($\epsilon = 1$), then:

$$R_\nu(\mu_c) = \frac{\frac{a}{2b}}{\frac{\mu_c}{3} - \frac{1}{2\sqrt{3}}} \quad . \qquad (3)$$

For illustrative purposes let us assume a/b = 0.6 and 0.1, for the cases of a weak and a strong temperature gradient, respectively, and let us consider how $W_\lambda/\Delta\lambda$ varies as a function of the fraction of the star over which the line is allowed to form. Thus one may construct Figure 8. This figure shows us that for lines formed only between the limb and, say, $\mu_c = 0.4$ there is a difference by a factor of 2 in the value of the equivalent width, with respect to what would be observed if the line

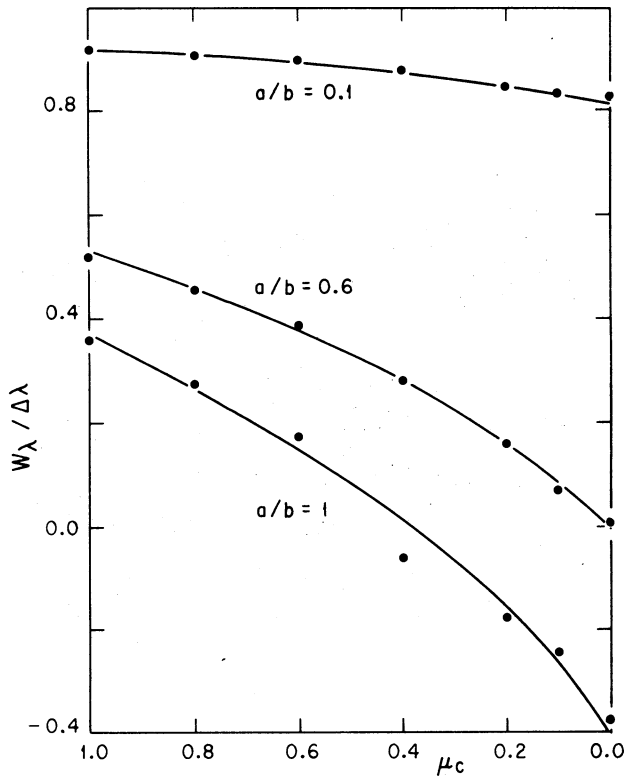

Fig. 8. The equivalent width of a pure absorption line as a function of the fraction of the star over which it is allowed to form. $\mu_c = 0$ corresponds to the poles while $\mu_c = 1$ corresponds to the entire surface.

were formed, under identical conditions, over the entire surface of the star. As one restricts the line formation region further, these factors increase.

Note that this is not applicable to the case of scattering lines ($\epsilon = 0$), which remain strong independently of μ.

If we return to the arguments used under the binary hypothesis, but now include this limb darkening effect, we find that, multiplying the equivalent widths of the N IV line in HD 193077 (Table 7) by a factor of 2 leads to equivalent widths which are practically the same as those in 10 Lac, implying that there may be only one continuum emitting source in HD 193077; that is, if the N IV 1687 line is formed preferentially in the polar regions and it is a pure absorption line HD 193077 is very likely to be a single object.

However, the picture which emerges when other lines are considered c.f. the Fe V lines in Table 7) is quite different, where factors of up to 10 would be needed to make the equivalent widths of HD 193077 and 10 Lac comparable (but note that this holds for the O-star companion of V444 Cyg as well).

The solution of this problem requires the results

an appropriate rotating model atmosphere, such those which have been constructed for Be stars e, c.f., review by Cassinelli 1987), and in which detailed treatment of the line transfer processes r different lines should allow for a more realistic ediction of the observed spectrum.

VI. CONCLUSIONS

The conclusions of this investigation are:

1) The *UV* emission line spectrum is dominated V + Fe VI blends. Most of the weakest features n be attributed to Fe IV, Fe III, Si III and P II and III.

2) There is a rich variety of interstellar lines esent in this spectrum, including numerous mponents of the higher degree of ionization lines ıich are shifted by -45 km s^{-1}, on the average.

3) The photospheric absorption line spectrum, ough difficult to measure accurately, includes ıes of Fe V, Fe IV, N IV, N III, Ni IV, and Si . A progression in FWCI is observed in the sense at the higher degree of ionization lines are much ırrower that those of lower degrees of ionization, nsistent with the presence of a rapidly rotating ar.

4) It is pointed out that (pure absorption) lines rmed only in the polar regions of a star will be eaker than those formed in a non-rotating star of uivalent temperature and gravity due simply to nb darkening. This leads to the possibility that ere is indeed only one star in HD 193077, as iginally proposed by Massey (1980), although a etailed rotating model atmosphere calculation is quired before the binary hypothesis is discarded.

Fitzpatrick (1982) emphasized the potential importance of a careful analysis of the photospheric lines present in many WR spectra. Indeed, there are veral problems which may be addressed through ıese data. In particular, we really know very little out the O-star companions to WR binaries, while is the properties of these companions which have, ıus far, been the cornerstone for the determination f the characteristics of the WR stars. In the case of D 193077, if it is a binary, the enormous rotation ıte in the O-star is unprecedented. If it is not a inary, then we have direct evidence that rotation ıight be involved in at least initiating the mass outows (as originally proposed by Limber 1964 and ıodeled by Sreenivasan and Wilson 1982).

It is interesting to note that intrinsic polarization expected among the effects produced as a consequence of rapid rotation (Sonneborn 1982), and is expected to vary as a function of wavelength. VR stars are known to have intrinsic polarization ı both continuum and emission lines (c.f. Robert *et l.* 1989, and references therein). Other interesting ffects of rotation on the atmospheres are reviewed by Cassinelli (1987) in relation to the Be stars, and may be applicable to the case of this system.

We wish to express our gratitude to the IUE and GSFC/RDAF staff, as well as to J. Nichols-Bohlin, R. Panek, G. Sonneborn and A. Warnock whose assistance and suggestions have been vital for this investigation. The archival data was extracted from the NSSDC. The figures were prepared by A. García and the final text by J. Orta. The completion of this work was made possible by the satellite link from the UNAM to the NSF TCP/IP network at NCAR.

REFERENCES

Adelman, S. and Leckrone, D.S. 1985, *IUE NASA Newsletter* No.28, 35.
Annuk, K. 1989, *Eesti NSV Teaduste Akadeemia Füüsika ja Astronoomia Osarond.*
Auer, L.H. and Koenigsberger, G. 1989, in *Proceedings of the Hot Star Workshop*, Garmany and Conti, eds., p. 291.
Boggess, A. *et al.* 1978a, *Nature*, **275**, 372.
Boggess, A. *et al.* 1978b, *Nature*, **275**, 337.
Bromage *et al.* (1982) *Third IUE Conference, Madrid*, p. 269.
Bruegeman, O. and Crenshaw, D.M. 1989, *IUE NASA Newsletter, No. 37*, 36.
Cassinelli, J.P.1987, in *Physics of Be Stars*, eds. A. Slettebak and T.P. Snow (Cambridge: Univ. Press), p. 106.
Conti, P.S. and Ebbets, D.C. 1977, *Ap.J.*, **213**, 438.
Dean, C.A. and Bruhweiler, F.C., 1985, *Ap.J. Suppl.*, **57**, 133.
Drechsel, H., Rahe, J., Kondo, Y., and McCluskey, G.E. 1981, *Astr. and Ap. Suppl.*, **45**, 473.
Ekberg, O. 1975a, *Phys. Scripta*, **12**, 42.
Ekberg, O. 1975b, *Phys. Scripta*, **11**, 23.
Ekberg, O. and Edlen, B. 1978, *Phys. Scripta*, **18**, 107.
Feibleman, W.A. and Bruhweiler, F.C. 1989, *Ap. J.*, **347**, 901.
Fitzpatrick, E.L. 1982, *Ap. J. (Letters)*, **261**, L91.
Grady, C.A. and Gerhart, M.P. 1989, *IUE NASA Newsletter No. 37*, 102.
Hiltner, W.A. and Schild 1966, *Ap. J.*, **143**, 770.
Hutchings, J.B. 1976, *Pub. A.S.P.*, **88**, 5.
Kelly, R.L. and Palumbo, L.J. 1973, *Atomic and ionic Emission Lines Below 2000 Å, NRL Report 7599.*
Koenigsberger, G. 1983, Ph. D. Thesis, The Pennsylvania State University.
Koenigsberger, G. 1986, *New Insights in Astrophysics*, ESA SP 263, p. 393.
Koenigsberger, G. 1988, *Rev. Mexicana Astron. Astrof.*, **16**, 75.
Koenigsberger, G. and Auer, L.H. 1985, *Ap. J.*, **297**, 255.
Koenigsberger, G. and Auer, L.H. 1987a, *Rev. Mex. Astron. Astrof.*, **14**, 271.
Koenigsberger, G. and Auer, L.H. 1987b, *Rev. Mex. Astron. Astrof.*, **14**, 277.
Lamontagne, R. 1983, Ph. D. Thesis, University of Montreal.
Lamontagne, R., Moffat, A.F.J., Koenigsberger, G., and Seggewiss, W. 1982, *Ap. J., 253*, 230.
Limber, N. 1964, *Ap. J.*, **139**, 1251.

Maeder, A. 1983, *Astr. and Ap.*, **120**, 113.
Massey, P. 1980, *Ap. J.*, **236**, 526.
Meyer, J.-P. 1985, *Ap. J. Suppl.*, **57**, 173.
Mihalas, D. 1978, *Stellar Atmospheres*, p. 314.
Moffat, A.F., Lamontagne, R., Shara, M., and McAlister, H.A. 1986, *A.J.*, **91**, 1392.
Nugis, T. and Sapar, A. 1985, *Soviet Astron. Lett.*, **11**, 188.
Pollock, A.M.T. 1987, *Ap. J.*, **320**, 283.
Prinja, R.K. and Howarth, I.D. 1986, *Ap. J. Suppl.*, **61**, 357.
Reader, J., Corliss, C.H., Wiese, W.L., and Martin, G.A. 1980, *Wavelengths and Transition Probabilities for Atoms and Atomic Ions*, U.S. Department of Commerce, NBS 68.
Robert, C., Moffat, A.F.J., Bastien, P., Drissen, L., and St.-Louis, N. 1989, *Ap. J.*, **347**, 1034.
Smith, P.L. 1987, in *Astrochemistry, IAU Symposium No. 120*, eds. M.S. Varya and S.P. Tarafdar, p. 95.
Sonneborn, G.H. and Collins II, G.W. 1977, *Ap. J.*, **213**, 787.
Sonneborn, G.H. 1982, in *Be Stars, IAU Symposium No. 98, eds. M. Jaschek and H.G. Groth, p. 493.*
Sonneborn, G., Oliverson, N.A., Imhoff, C.L., Pitts, R.E., and Holm, A.V. 1987, *IUE Observing Guide*, NASA IUI Newsletter, p. 45.
Sreenivasan, S.R. and Wilson, W.J.F. 1982, *Ap. J.* **254**, 287. Striganov, A.R. and Svetitskii, N.S. 1968 *Tables of Spectral Lines of Neutral and Ionized Atoms* IFI/PLENUM, N.Y. Washington.
Striganov, A.R. and Svetitskii, N.S. 1968, *Tables of Spectra Lines of Neutral and Ionized Atoms*, IFI/PLENUN, N.Y. Washington.
St. Louis, N., Moffat, A.F.J., Drissen, L., Bastien, P., and Robert, C. 1988, *Ap. J.*, **330**, 286.
van der Hucht, K.A., Conti, P.S., Lundström, I., and Stenholm, B. 1981, *Space Sci. Rev.*, **28**, 227.
Walborn, N.R., Nichols-Bolin, J., and Panek, R. 1985 *IUE Atlas of O-type Spectra from 1200 to 1900 A*, NASA Publ. 1155.
Wannier, P.G., Penzias, A.A., and Jenkins, E.B. 1982, *Ap J.*, **254**, 100.
Willis, A.J. and Stickland, D.J. 1983, *M.N.R.S.*, **203**, 619
Willis, A.J., van der Hucht, K.A., Conti, P.S., and Garmany, C. 1986, *Astr. and Ap. Suppl.*, **63**, 417.
Willis, A.J., Howarth, I.D., Stickland, D.J., and Heap, S.R 1989, *Ap. J.*, **347**, 413.

Gloria Koenigsberger: Instituto de Astronomía, Apartado Postal 70-264, 04510, México, D.F., México.